The Q_{weak} Experiment: Its Physics Significance and Legacy

Donald Jones

Department of Physics
University of Virginia
Charlottesville, VA 22904, USA

Seminar July 2015

Brief History of Parity-Violating Neutral Current Physics

1967– Steven Weinberg published model of electroweak theory including unobserved PV weak neutral currents.

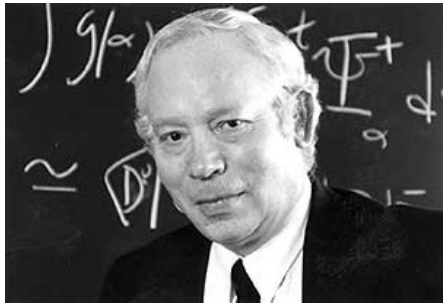

1973– First weak neutral event observed in bubble chamber (Gargamelle).
1978– E122 at SLAC (Prescott *et al.*) confirms parity violation in neutral weak currents.

Parity violation established as a physics probe:

- Nuclear and nucleonic structure:
  - Strange quark program: HAPPEX I-III and G0(JLab), SAMPLE(Bates), A4(Mainz)
  - Neutron skin: PREX (JLab)
- Lepton and quark couplings: E158 and Qweak
- SM Tests:
  - E158, Qweak
  - Future, P2, SOLID program, MOLLER

Parity Violation Defined

Any process that is **not** invariant under a parity transformation is said to violate parity.
So any physical observable measured to be different between two experiments, identical with the exception of a parity inversion, violates parity.

- Signature of the weak force
- Arises from structure of weak interaction mixing axial vector and vector components:

$$\overline{u}\gamma_\mu(g_v - g_A\gamma_5)u$$

- Rotational invariance of law of physics means parity inversion = mirror image
- Longitudinally polarized electron scattering→ parity inversion = flip of electron helicity ($Helicity = \mathbf{S}\cdot\mathbf{p}$)

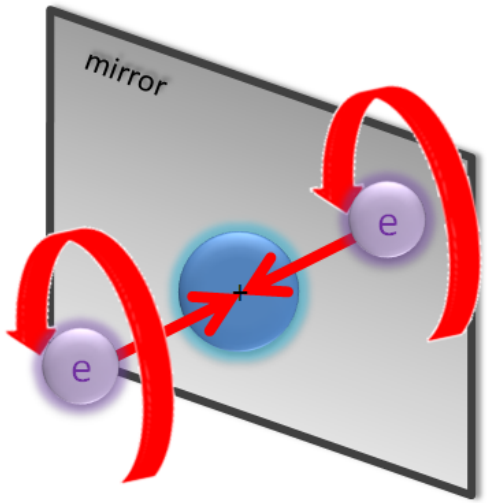

Introduction to Qweak

- Measuring the proton weak charge by elastic ep scattering (polarized electrons on a liquid hydrogen (LH_2) target).
- Determine weak charge from asymmetry of scattering rates of + and – helicity electrons.
- Parity violating asymmetry arises from interference between EM and neutral weak scattering amplitudes.

$$\sigma \propto |M_\gamma + M_Z|^2 \approx |M_\gamma|^2 + 2M_\gamma^* M_Z$$

$$A_{PV} \sim \frac{2|M_\gamma^* M_z^{PV}|}{|M_\gamma|^2}$$

$$\boxed{A_{PV}|_{Q^2=0} \propto Q_W^p}$$

$$A_{ep} = \frac{\sigma_+ - \sigma_-}{\sigma_+ + \sigma_-}$$

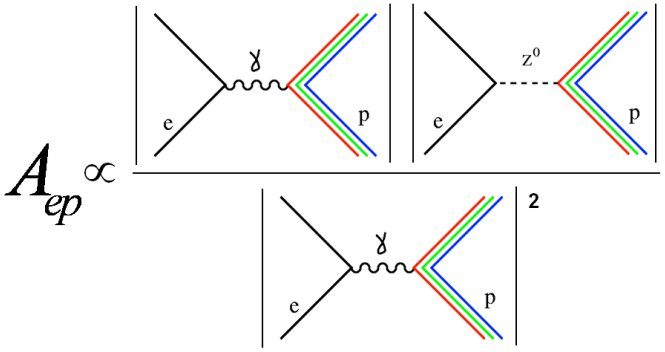

Qweak Sensitivity to New Physics

- Q_W^p is accidentally suppressed and precisely predicted by the SM. Good candidate for a new physics search.
- Contact interactions ($Q^2 << M^2$) the physics takes a simple form
- New physics in terms of effective contact interaction with mass scale Λ and coupling g

$$\mathcal{L} = \mathcal{L}_{SM}^{PV} + \mathcal{L}_{New}^{PV}$$

$$\mathcal{L}_{SM}^{PV} = -\frac{G_F}{\sqrt{2}} \bar{e}\gamma_\mu\gamma_5 e \sum_q C_{1q}\bar{q}\gamma^\mu q$$

$$\mathcal{L}_{New}^{PV} = \frac{g^2}{4\Lambda^2} \bar{e}\gamma_\mu\gamma_5 e \sum_q h_V^q \bar{q}\gamma^\mu q$$

- Qweak sensitive certain models of new physics at TeV scales, e.g. Z', SUSY, leptoquarks.

	Q_{EM}	Q_{weak}(1st order)
q_u	$+\frac{2}{3}$	$+1 - \frac{8}{3}sin^2\theta_W \approx +0.383$
q_d	$-\frac{1}{3}$	$-1 + \frac{4}{3}sin^2\theta_W \approx -0.695$
p	$+1$	$+1 - 4sin^2\theta_W \approx +0.074$
n	0	-1

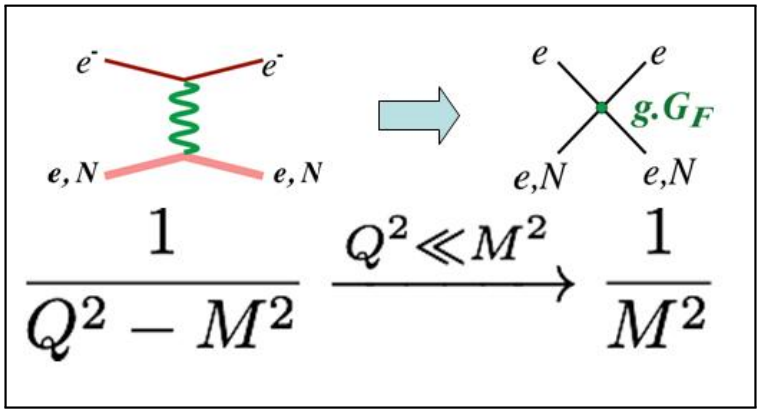

Qweak Sensitivity to VA and AV Couplings

- The electroweak contact interaction can be expressed in terms of the axial vector-vector (AV) and vector-axial vector (VA) coupling constants C_{1q} and C_{2q} used in low energy precision physics.
- Qweak sensitive to C_{1q}'s (AV)
  $$Q_W^p = -2(2C_{1u} + C_{1d})$$
- Different sensitivities to orthogonal isospin combinations of couplings
  isoscalar:$(C_{1u} + C_{1d})$
  isovector:$(C_{1u} - C_{1d})$
- Atomic parity violating (APV) physics ($N_u \approx N_d$) and PVES provide complementary measurements.
- PVES more sensitive to isovector.

$$\bar{f}\gamma_\mu(g_V - g_A\gamma_5)f$$

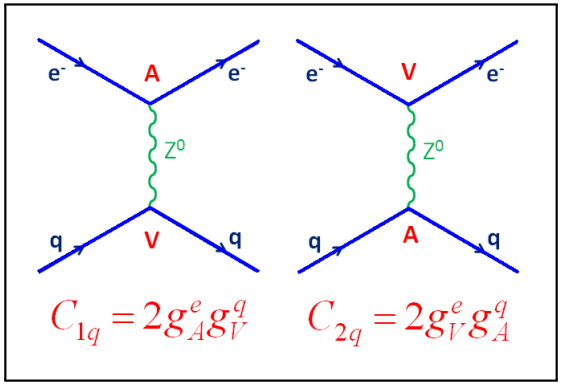

Small θ Large θ

	Q_{EM}	Q_{weak}(1st order)
q_u	$+\frac{2}{3}$	$+1 - \frac{8}{3}sin^2\theta_W \approx +0.383$
q_d	$-\frac{1}{3}$	$-1 + \frac{4}{3}sin^2\theta_W \approx -0.695$
p	$+1$	$+1 - 4sin^2\theta_W \approx +0.074$
n	0	-1

Qweak Published Results Constrain Quark Weak Charges

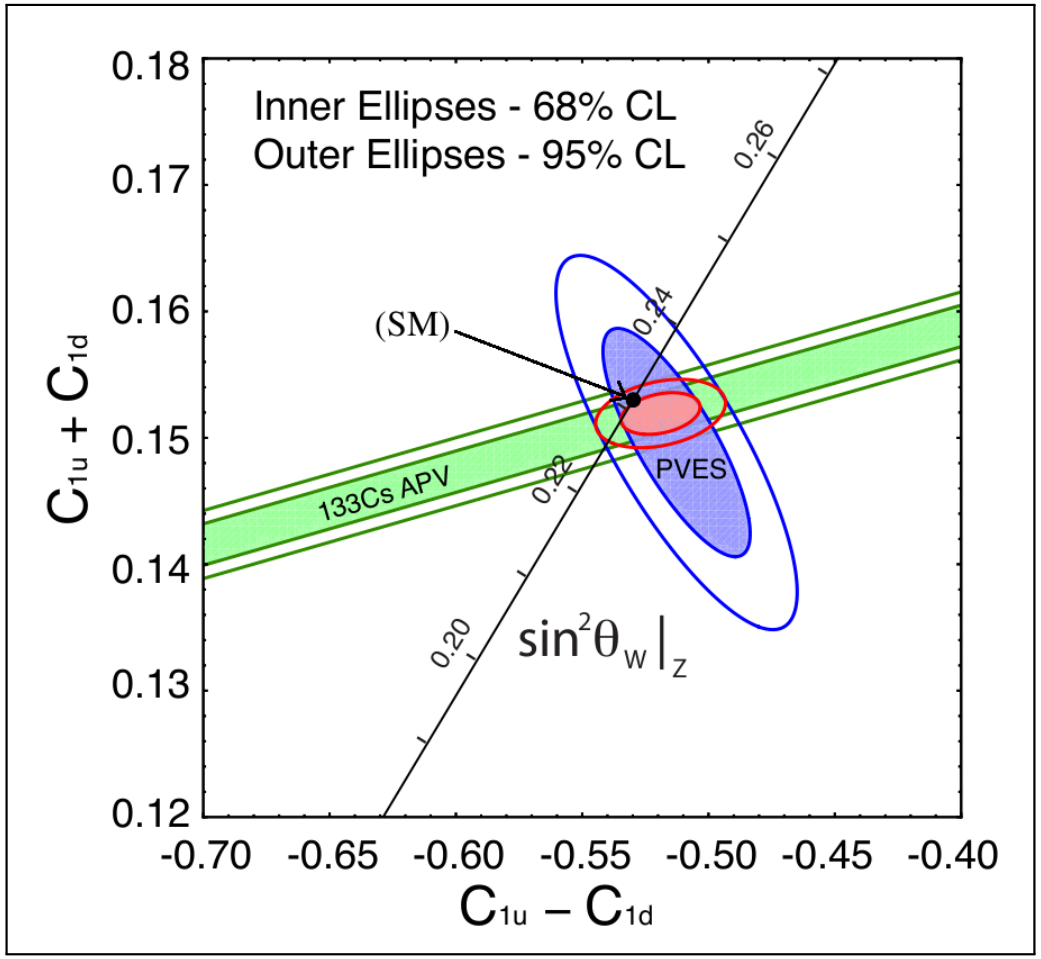

Recently published results of global fit to world data including 4% of Qweak data set[1].

[1] *First Determination of the Weak Charge of the Proton.* Phys. Rev. Lett. 111, 141803 (2013)

Extraction of Q_W^p

PVES data points shown on this plot have been extrapolated to $\theta = 0$ using global fit. Uncertainties arising from fit are shown as additional error bars.

Plot of World Parity Violating ep Data for Asymmetry vs Q^2

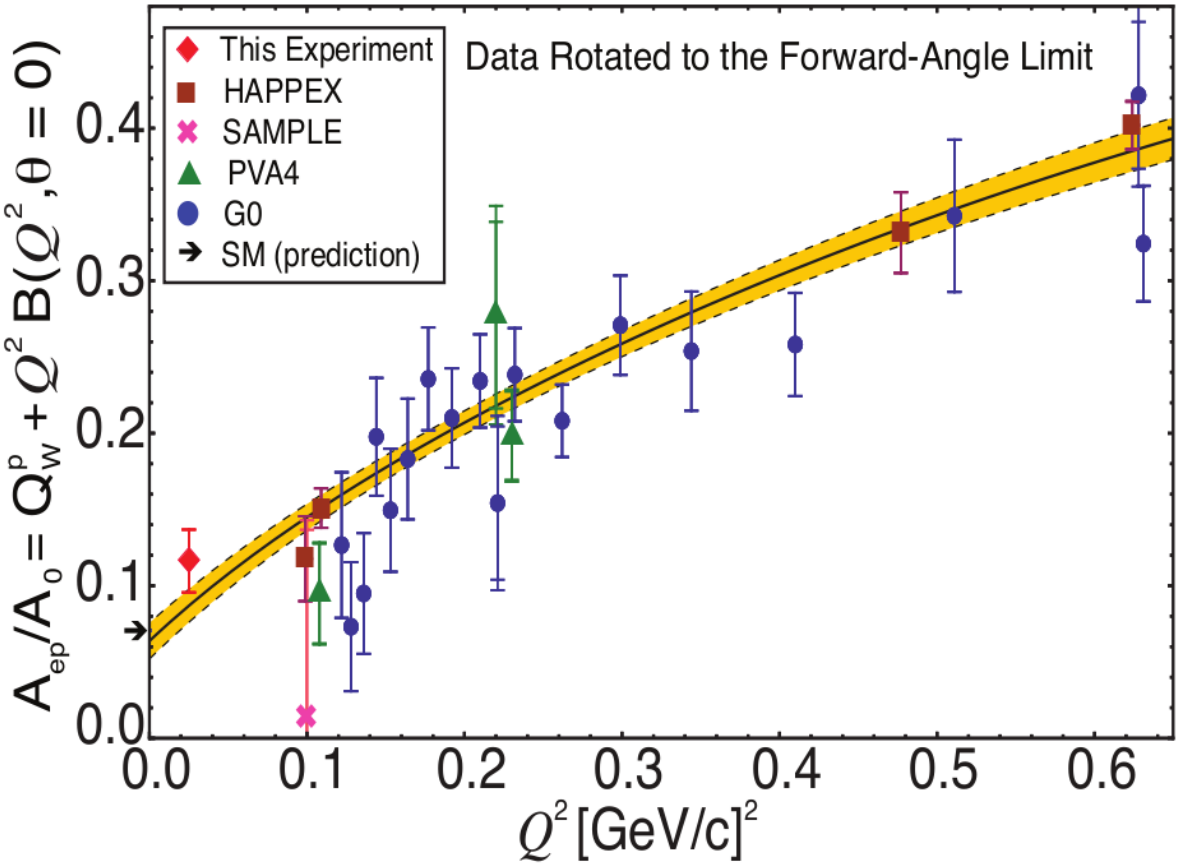

Extraction of Q_W^p

$$A_{PV}/A_0 = Q_W^p + Q^2 B(Q^2, \theta)$$

- Global fit of PVES data on hydrogen, helium, deuterium and ^4He was used to extract Q_W^p– Qweak, G0, HAPPEX, SAMPLE, PVA4.
- Effectively five parameters used in fit:
  –weak charges C_{1u} and C_{1d}
  –strange charge radius ρ_s and magnetic moment μ_s
  –isovector axial form-factor $G_A^{Z\ (T=1)}$ (isoscalar form factor $G_A^{Z\ (T=0)}$ constrained[1]).
- Energy dependent electroweak correction from $\Box_{\gamma z}$ made at kinematics of each experiment before fit.
- Resulting fit is $A_{PV}(\theta, Q^2)$
- Q_W^p taken as the intercept of fit of $A_{PV}/A_0|_{\theta=0}$ vs Q^2.

[1] S.L. Zhu, S.J. Puglia, B.R. Holstein and M.J. Ramsey-Musolf, Phys. Rev. D 62, 033008 (2000).

Qweak Published Results

Recent PRL publication of Qweak results including 4% of the full data set. The result including world data is a 19% determination Q_W^p.

Qweak Asymmetry Result	Fit to World PVES Data
$A_{PV} = -279 \pm 35(stat) \pm 31(sys) ppb$	$Q_W^p = +0.064 \pm 0.012 \quad (SM + 0.0710)$ $Q_W^n = -0.975 \pm 0.010 \quad (SM - 0.9890)$

Parameters used in this determination. Final result will require much more precision.

E_{beam} Pol	$89.0 \pm 1.8\%$	Moller Polarimeter only
$\langle E_{beam} \rangle$	$1.155 \pm 0.001(GeV)$	Simulation and Measurement
$\langle Q^2 \rangle$	$0.0250 \pm 0.0006(GeV/c)^2$	Geant Simulations
θ_{eff}	7.90 deg	Simulation and Measurement

Qweak Main Apparatus Schematic

Production Mode
–high current 180 μA

Tracking Mode
–low current 50 pA

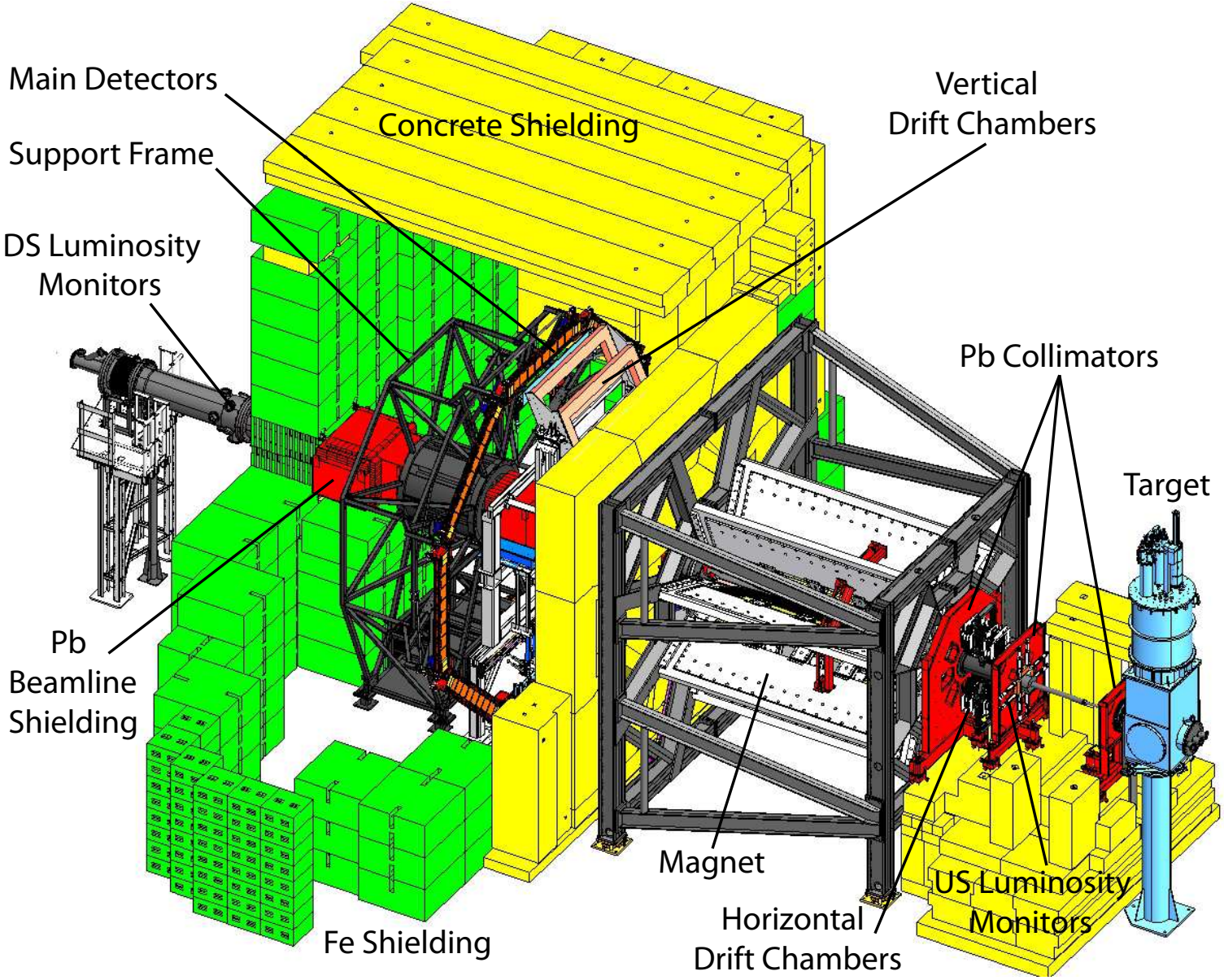

Qweak Installation Picture

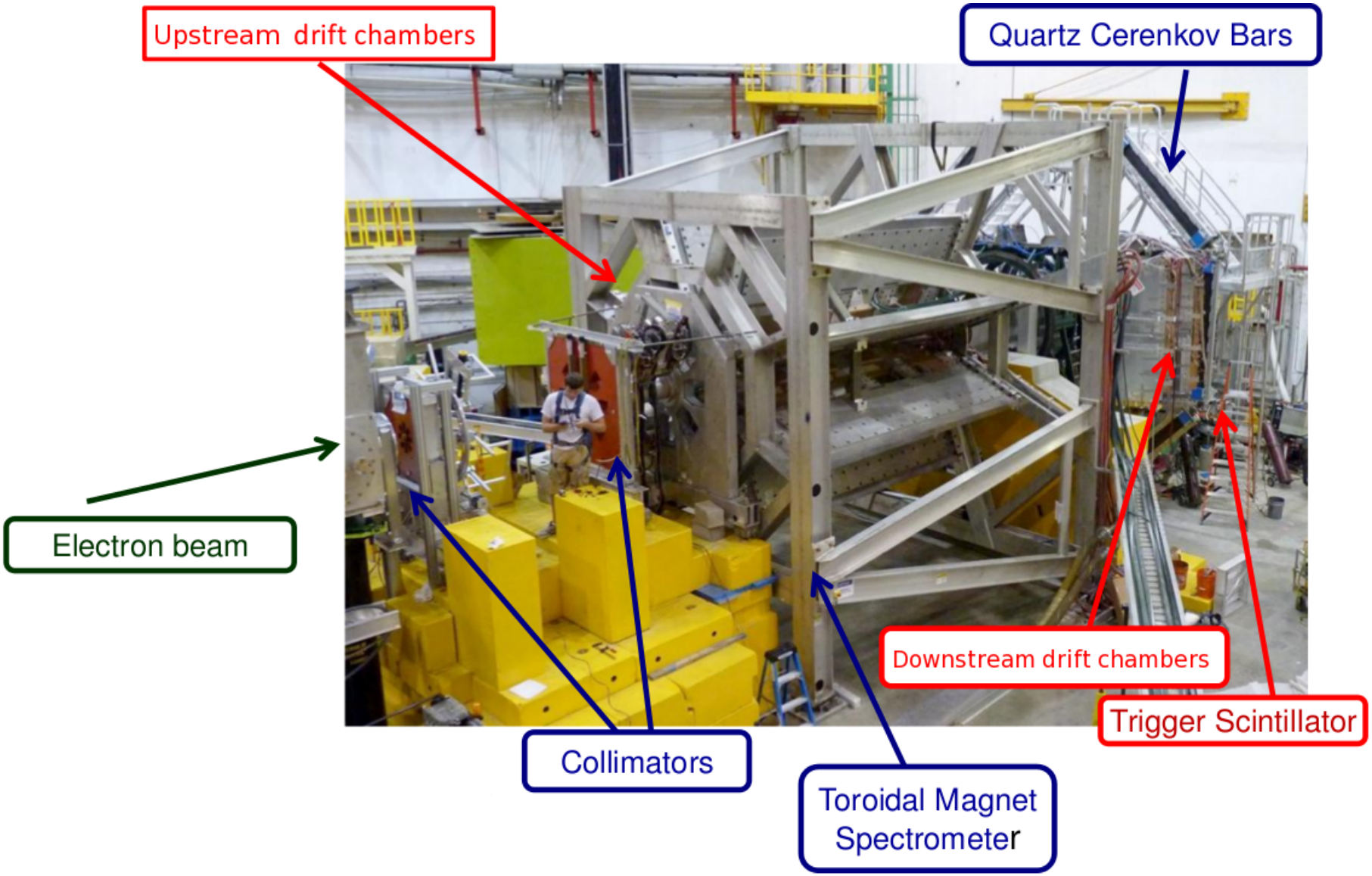

Statistical Challenges for Qweak

- Statistics
  - High polarization and current
  - High power target
  - Large acceptance detector = high rates
- Width Considerations
  - Total quartet asymmetry width 230 ppm
  - 2-3 billion quartets needed

Qweak Statistics Goals
$A_{PV} \approx 270\ ppb$
$\delta A_{PV} \approx \pm 2.1\%(5\ ppb)$
$\delta Q_W^p \approx \pm 4\%$
$\delta sin^2\theta_W \approx \pm 0.3\%$

Qweak's goal is the most precise relative and absolute PVES measurement to date.

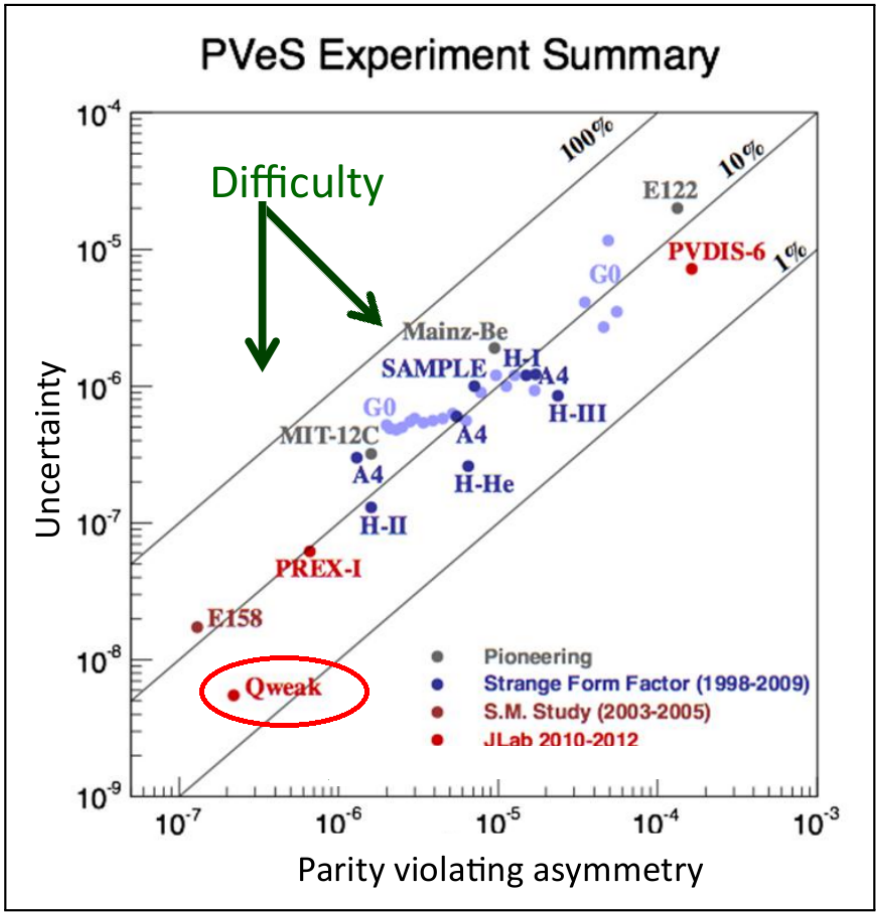

Qweak Main Detector

- 8 azimuthally symmetric fused silica quartz Čerenkov detectors with 2 cm Pb pre-radiators.
- 850 MHz per bar at 180 μA$\rightarrow$integrate
- Low noise electronics with 18 bit ADC with signal integration in FPGA.
  - Detector(215 ppm)
  - BCM resolution (44 ppm)
  - Target density fluctuations (55 ppm)
  - Electronics noise (5 ppm)

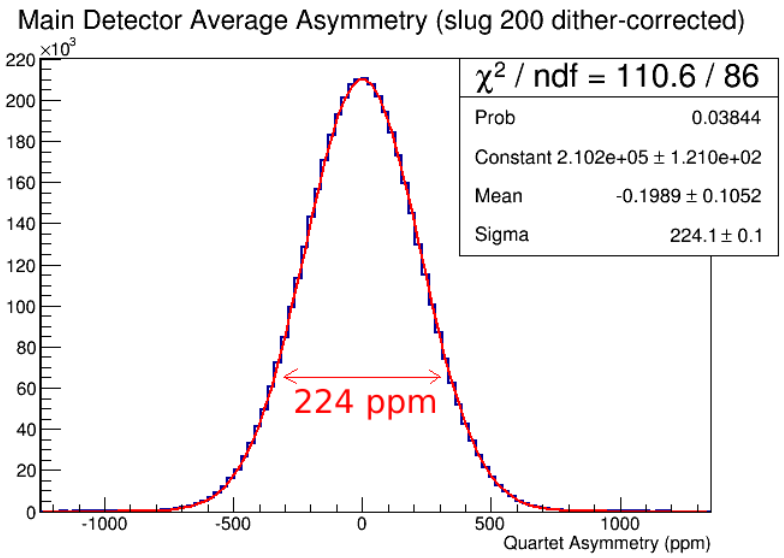

Detector bar installed.

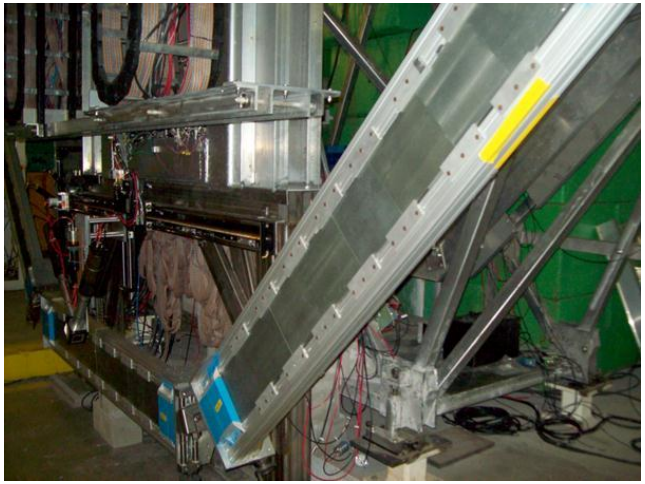

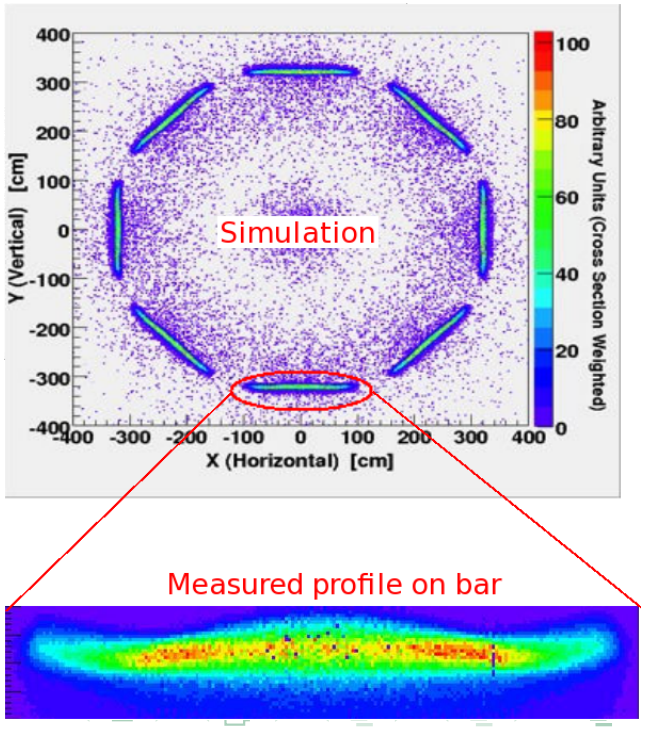

Systematic Challenges for Qweak

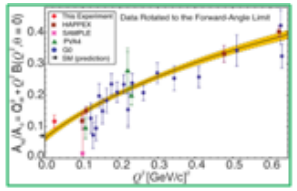

What we need→ $\frac{A_{PV}}{A_0} = Q_W^p + Q^2 B(Q^2, \theta), \qquad A_0 = \frac{-G_F Q^2}{4\pi\alpha\sqrt{2}}$

What we measure→ $A_{raw} = P\left(\frac{(1-\Sigma f_b)A_{PV}}{R} + \Sigma f_b A_b\right) + A_{beam} + A_T + A_\varepsilon$

e polarization

Background fraction
- aluminum windows
- diffuse neutral bkg
- inelastics

Correction accounts for energy losses in target and translation between $\langle A(Q^2)\rangle$ and $A(\langle Q^2\rangle)$

Background asymmetries

False asymmetries from HC beam properties

PV conserving asymmetry from transverse e-pol

False asymmetries from electronics

Systematic Challenges for Qweak

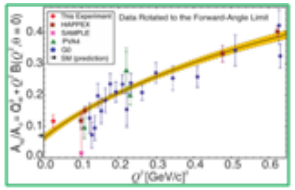

What we need→ $\frac{A_{PV}}{A_0} = Q_W^p + Q^2 B(Q^2,\theta), \qquad A_0 = \frac{-G_F Q^2}{4\pi\alpha\sqrt{2}}$

What we measure→ $A_{raw} = P\left(\frac{(1-\Sigma f_b)A_{PV}}{R} + \Sigma f_b A_b\right) + A_{beam} + A_T + A_\varepsilon$

Moller & Compton

e polarization

Background fraction
- aluminum windows
- diffuse neutral bkg
- inelastics

Tracking and Simulation

Correction accounts for energy losses in target and translation between $\langle A(Q^2)\rangle$ and $A(\langle Q^2\rangle)$

Background Detectors

Background asymmetries

False asymmetries from HC beam properties

Beam Modulation and Linear Regression

PV conserving asymmetry from transverse e-pol

Symmetric Cancellation and Minimization

False asymmetries from electronics

Null Channels

Polarimetry

Proposal allows $\pm 1\%$ uncertainty

- Moller: ee scattering off polarized iron foil
  Dedicated low current measurements
  Run 2 uncertainty $\pm 0.84\%$
- Compton: γe scattering from circularly polarized laser
  Continuous non-invasive[a] high current measurement
  Run 2 e-detector uncertainty $< 0.6\%$

MOLLER and PVDIS require $\pm 0.4\%$ polarimetry! Looks within reach.

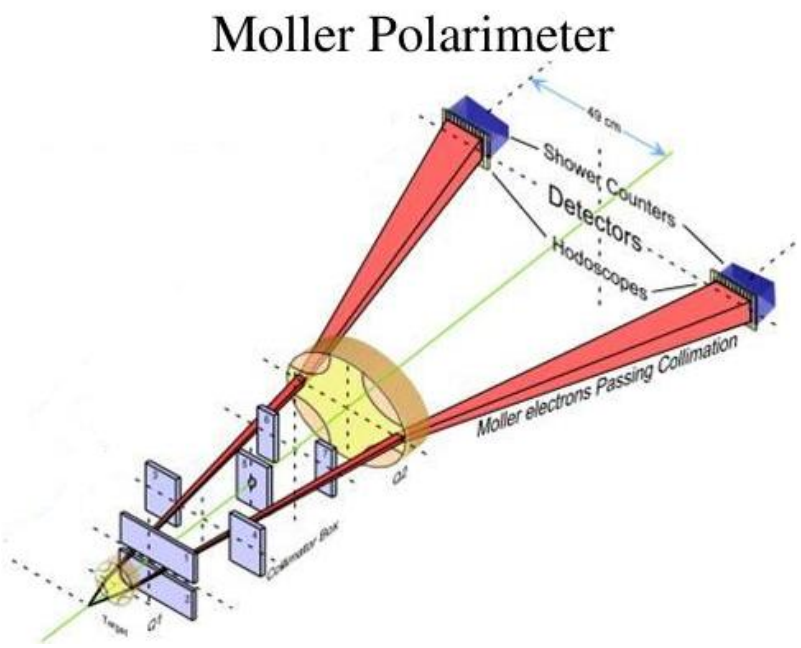

[a] May have to revisit this statement for MOLLER

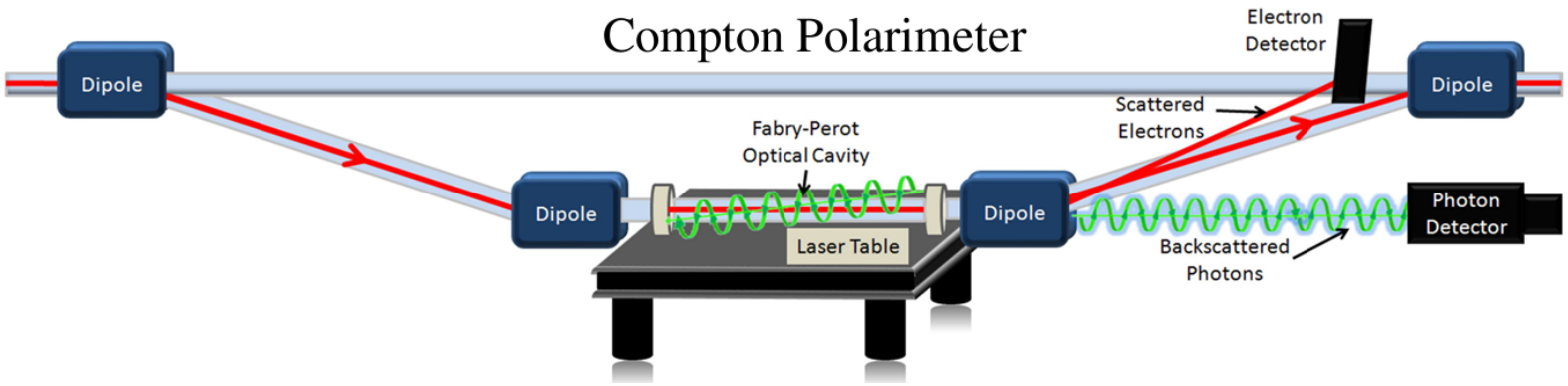

Electron Beam Polarization

Qweak polarimetry results taken over ∼6 months.

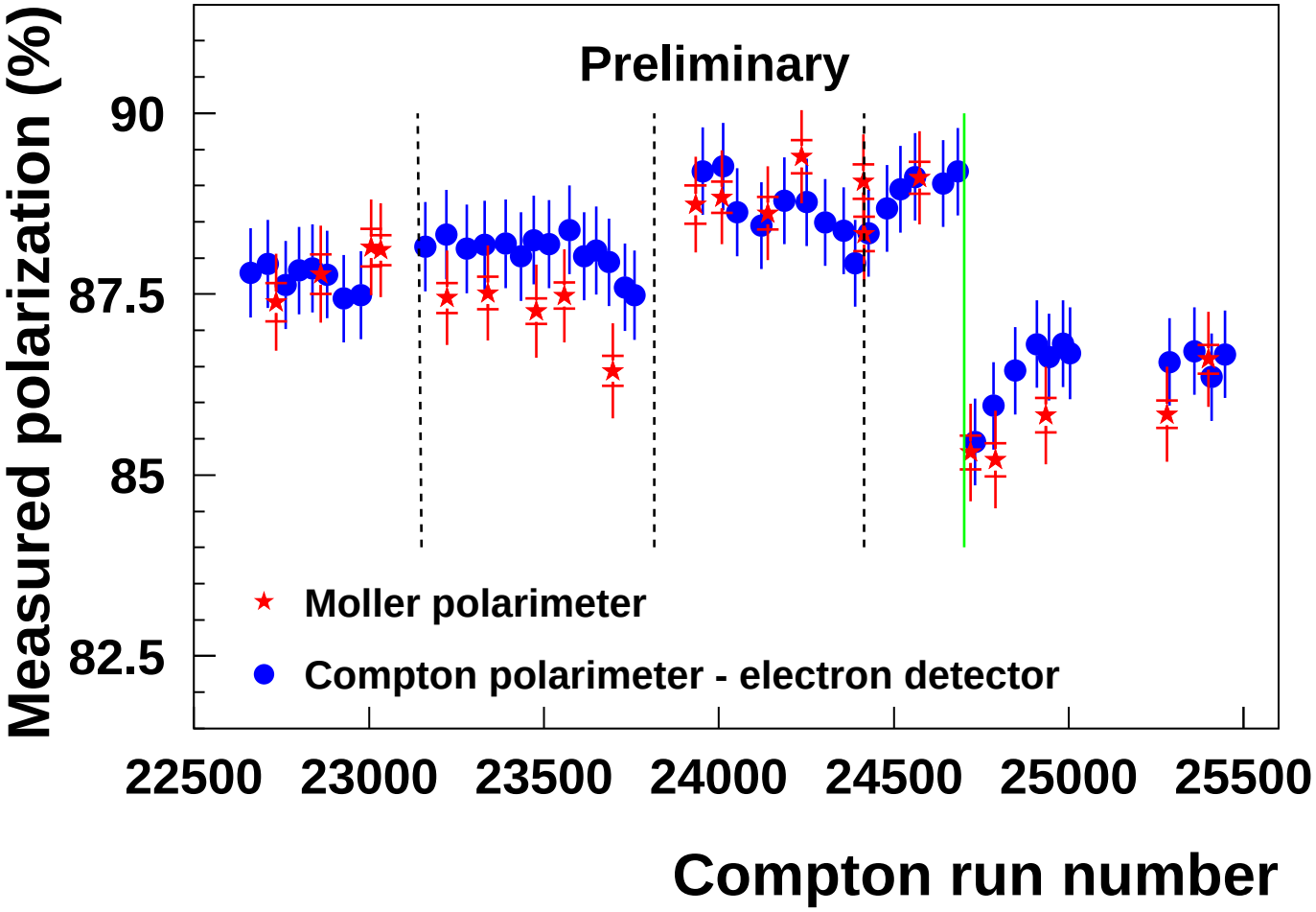

Compton Electron Detector

- Diamond microstrip electron detector
- Radiation hard 21mm x 21mm diamond planes with metalized strips:
  200 μm pitch–180 μm width and 20 μm gap
- Capture majority of Compton spectrum (7-5 mm from beam)
- Asymmetry formed strip by strip and spectrum shape fit

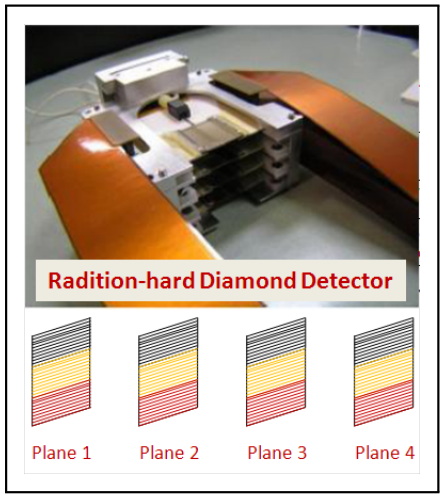

Electron Detector Asymmetry Spectrum

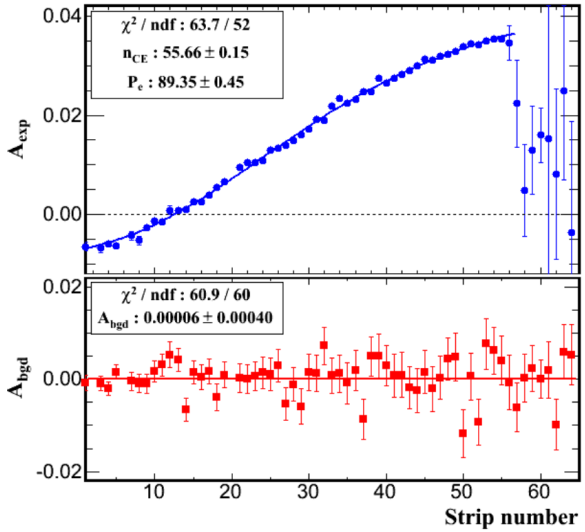

Electron Detector Plane 1 Yield (Rate) Spectrum

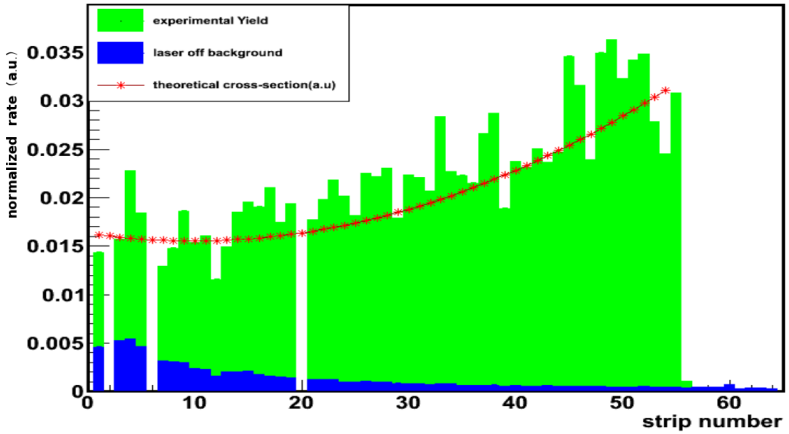

Compton Systematics

Run 2 Hall C Compton systematics.

Source	Uncer-tainty	$\Delta P/P$ (%)
Laser polarization	0.18%	0.18
Plane-to-plane	secondaries	0.00
3rd Dipole field	0.0011 T	0.13
Beam energy	1 MeV	0.08
Detector Z position	1 mm	0.03
Trigger multiplicity	1-3 plane	0.19
Trigger clustering	1-8 strips	0.01
Detector tilt (X)	1°	0.03
Detector tilt (Y)	1°	0.02
Detector tilt (Z)	1°	0.04
Strip eff. variation	0.0 - 100%	0.1
Detector Noise	$\leq$20% of rate	0.1
Fringe Field	100%	0.05
Radiative corrections	20%	0.05
DAQ ineff. correction	40%	0.3
DAQ ineff. pt-to-pt		0.3
helicity correl. beam pos.	5 nm	< 0.05
helicity correl. beam pos.	5 nm	< 0.05
chicane spin precession	20 mrad	< 0.03
Total		0.59

$$A_{meas} = P_\gamma P_e A_{theory}$$

- Laser degree of circular polarization (DOCP) was 100.00% (0.18%)
- Both LCP and RCP accessible at 100%
- Quadrature sum suppression of DOCP sensitivity to linear shifts
  $$DOCP = \sqrt{1 - DOLP^2}$$
- Hall A Compton quotes laser polarization at $\pm 0.8\%$[a]

[a] M. Friend *et al.*, Upgraded photon calorimeter with integrating readout for Hall A Compton Polarimeter at Jefferson Lab (2011)

Compton Laser Table Layout

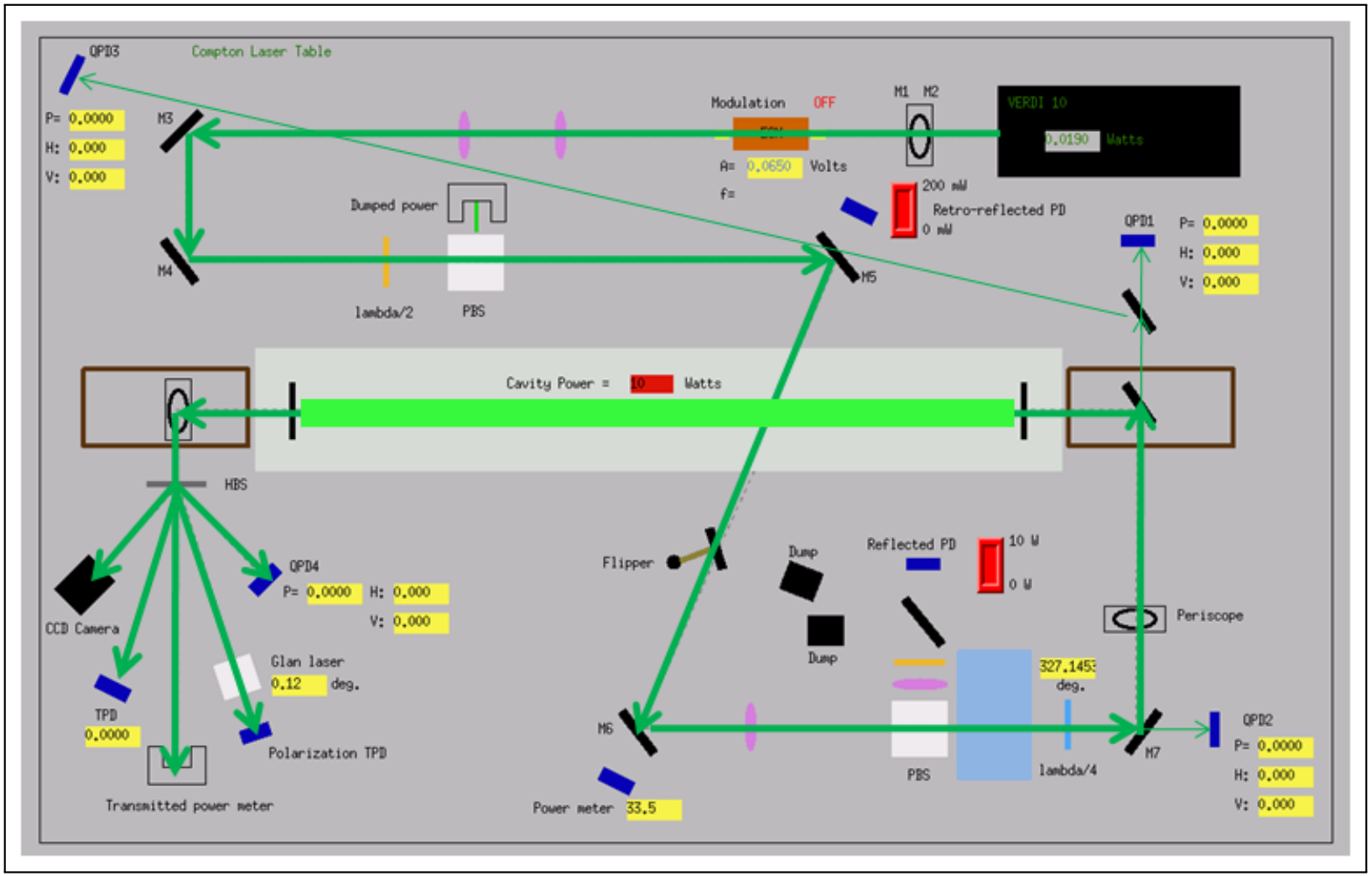

Measuring Transfer Matrix

Laser/cavity controls and analysis GUI shown here measuring exitline DOCP

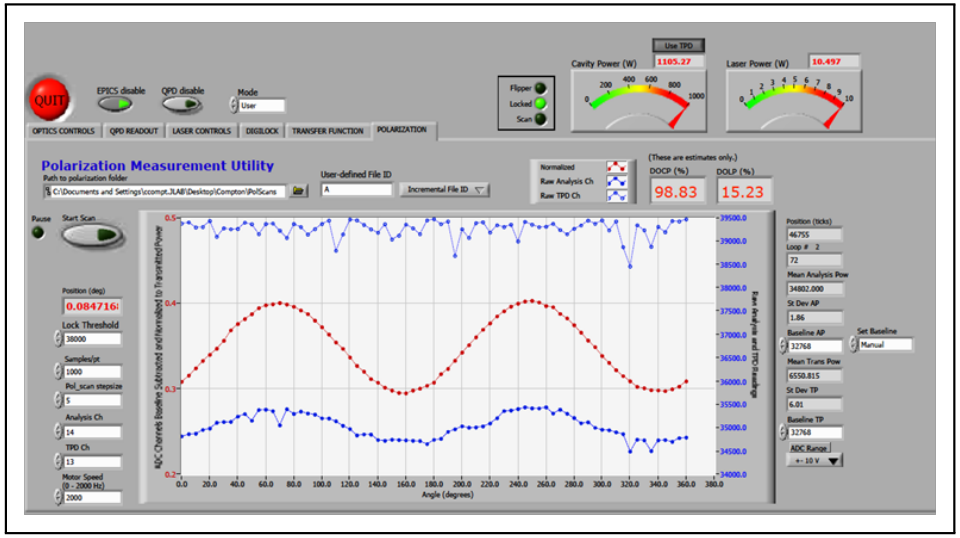

Usual Method

- Open cavity region of beam pipe
- Measure many identical polarization states inside the cavity and in the exit line
- Find transfer matrix (TM) to map exitline measurements back to cavity

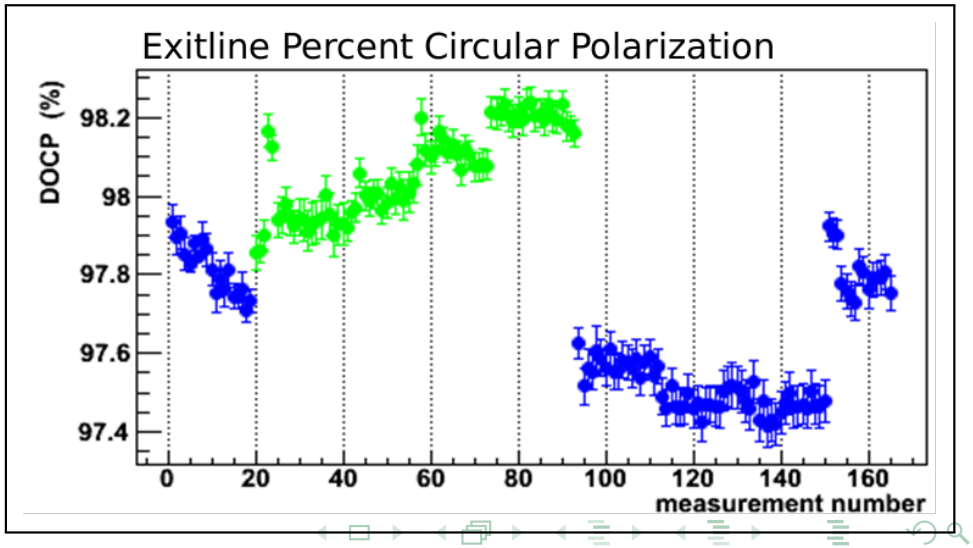

A Windows Problem Bill Gates Can't Fix

- Evidence for significant birefringence changes on vacuum windows
  - –Tightening flanges (Hall A design)
  - –Pulling vacuum
- TM changes after you close the cavity

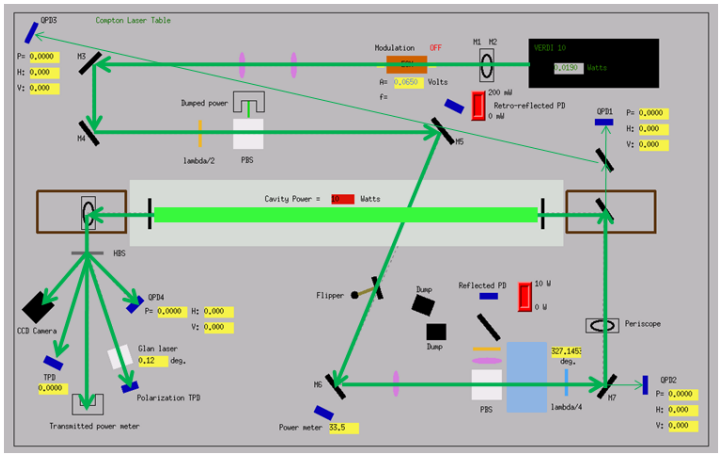

DOCP in exitline shown versus QWP angle (controls cavity input laser state). Input state maximizing DOCP in exitline changes with pressure on flanges showing TM is changing.

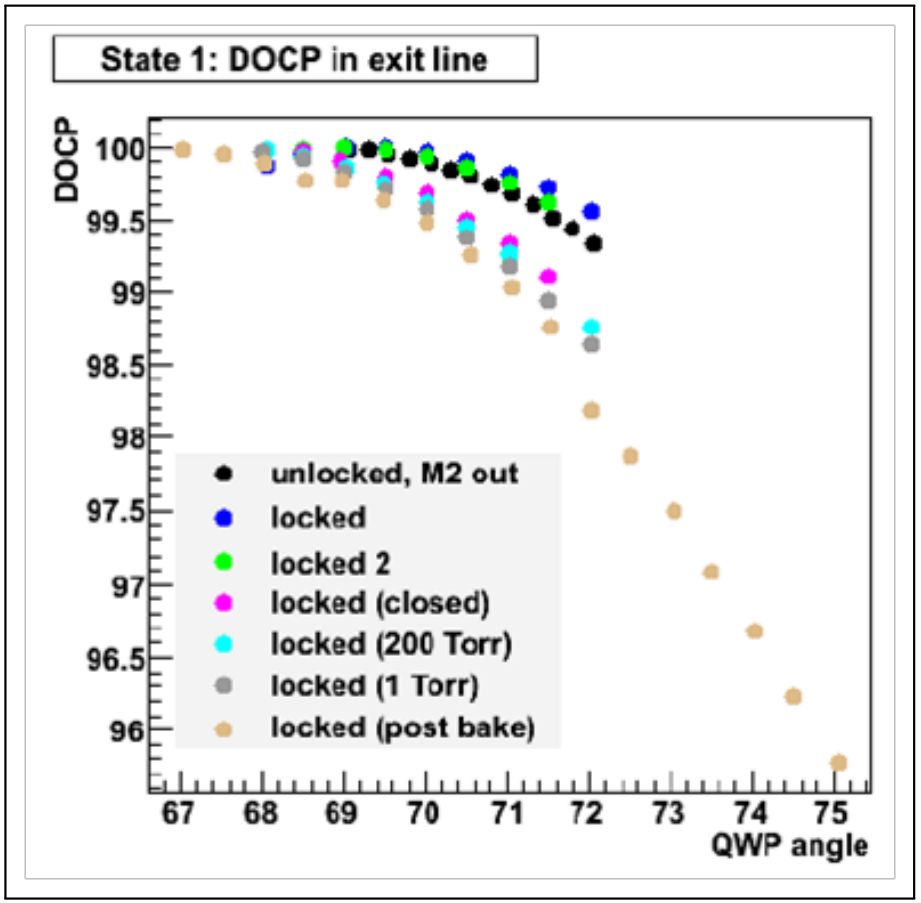

Phew! Solution found just before Run 2 Startup

Solution: add HWP and minimize leaked light

- Optical reversibility theorems relate DOCP at cavity input to power returning to laser head.
- 2nd year optics: LP + QWP = optical isolator
- $HWP_{rot} + QWP_{rot} + Vacuum\ Window = QWP_{perfecto}$

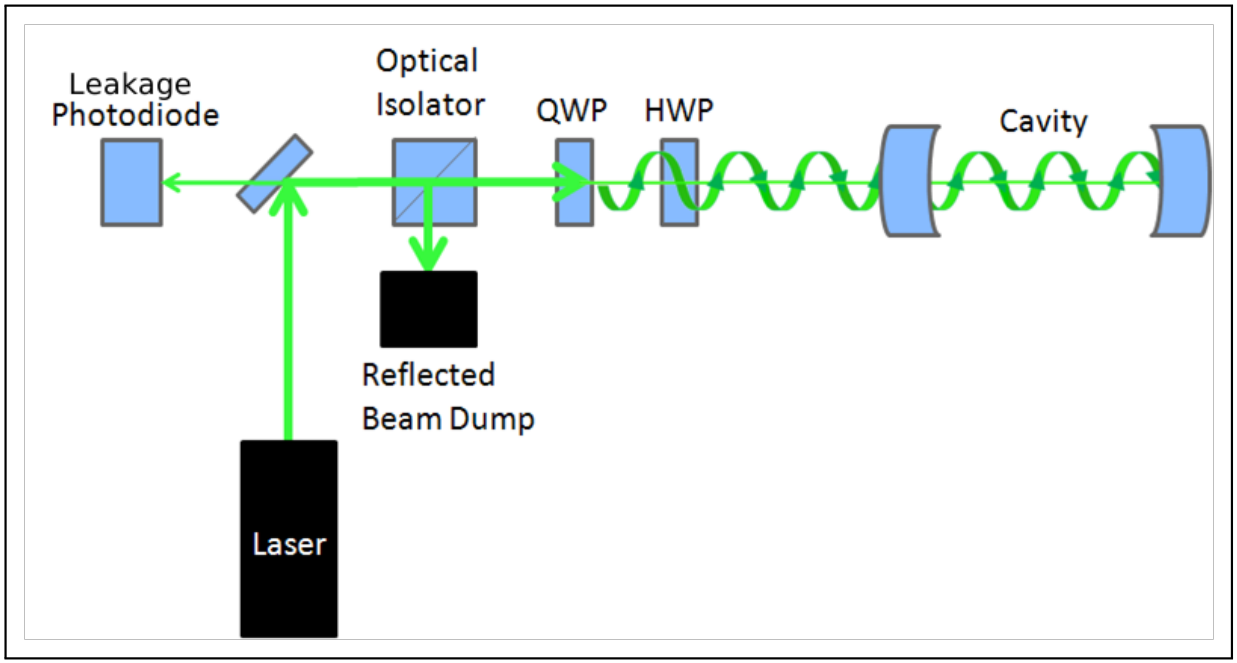

Scans of Reflected Leakage

- Measured leakage power vs HWP and QWP angles over full phase space.
- Fit to model gives DOCP in cavity (Right)
- Direct measurement inside cavity confirms model (Below)
- Correlation between leaked power and DOCP gives access to ~100% DOCP

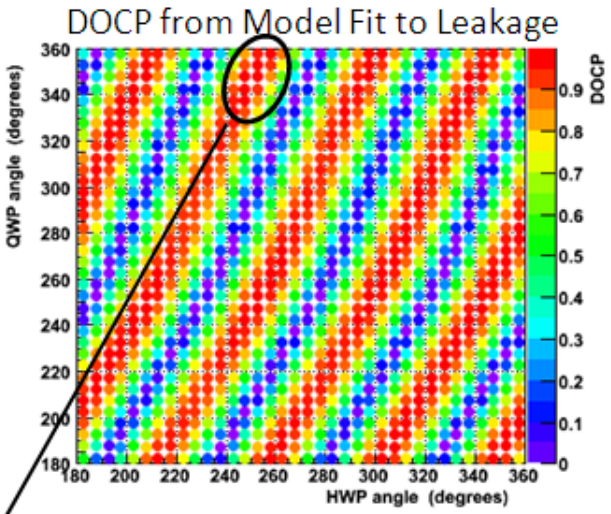

Results of direct test:

->Minimized reflection leakage
->Directly measured DOCP in cavity region

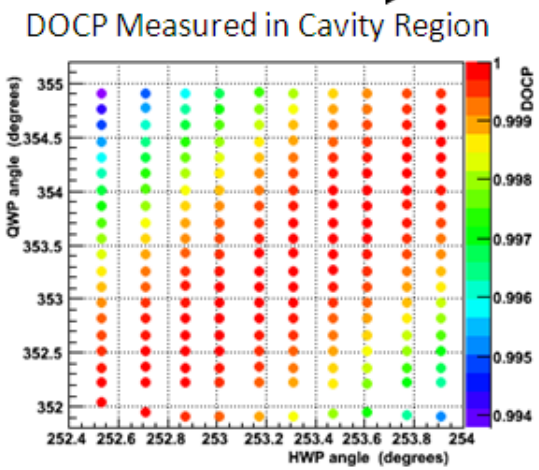

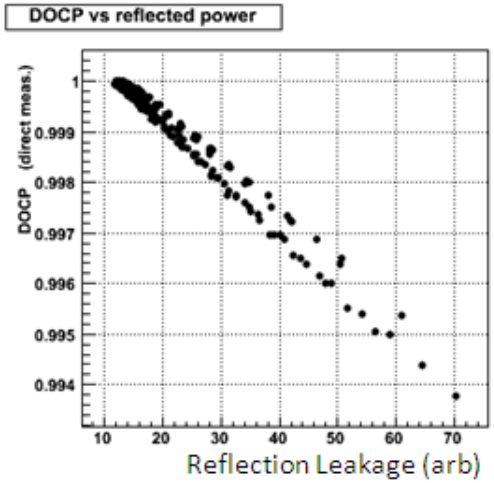

Tracking System

- Tracking system necessary for benchmarking simulation used to determine final Q^2.

$$\overline{A_{PV}} = \frac{A_{pv}}{A_0} = Q_W^p + Q^2 B(\theta, Q^2), \qquad A_0 = \frac{-G_F Q^2}{4\pi\alpha\sqrt{2}}$$

- Horizontal and vertical drift chambers for track reconstruction.
- Low currents (∼50pA) necessary for recording individual tracks.
- Geant 4 used to correct Q^2 for radiative effects and apply proper light weighting.

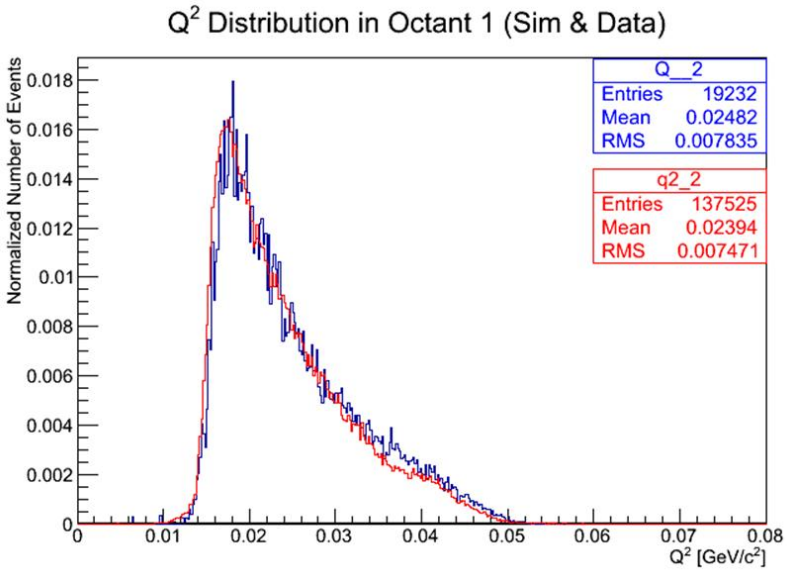

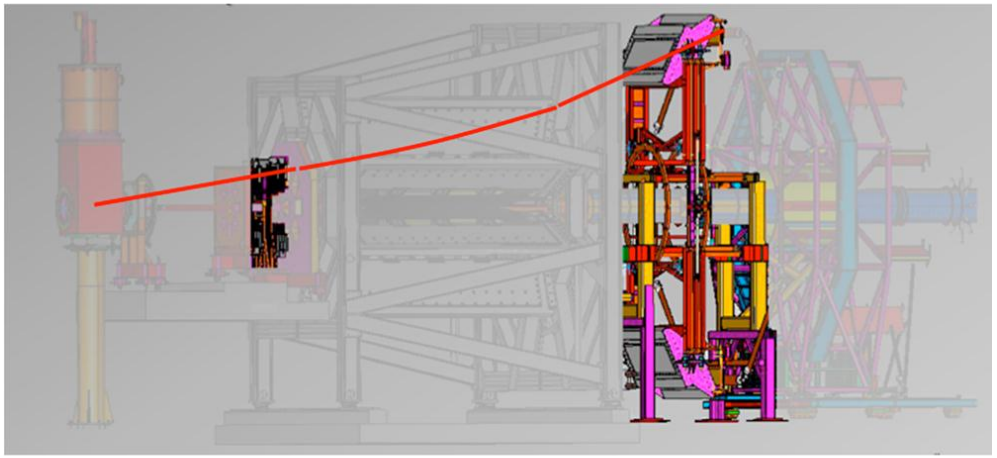

Tracking System

- Tracking system necessary for benchmarking simulation used to determine final Q^2.

$$\overline{A_{PV}} = \frac{A_{pv}}{A_0} = Q_W^p + Q^2 B(\theta, Q^2), \qquad A_0 = \frac{-G_F Q^2}{4\pi\alpha\sqrt{2}}$$

- Horizontal and vertical drift chambers for track reconstruction.
- Low currents ($\sim$50pA) necessary for recording individual tracks.
- Geant 4 used to correct Q^2 for radiative effects and apply proper light weighting.

Optimistic about meeting the proposed $\pm 0.5\%$ uncertainty on Q^2.

Requires 5x improvement from published Run 0 results

Removal of Background Asymmetries: Aluminum Windows

Qweak's largest background and largest correction comes from Al target windows.

$$\text{Correction} = f_{Al} A_{Al} / (1 - \sum f_i) \approx -58\ ppb\ (\sim 30\% \text{ of } A_{PV})$$

Factional Rate from Windows

- Fraction of signal from aluminum windows $f_{Al} \approx 3\%$
- Fraction measured comparing event mode rates of full and evacuated target (corrected for radiative effects of LH_2)

Aluminum PV Asymmetry

- Asymmetry measured from thick Aluminum dummy target.

$$A_{Al} \approx 1.8\ ppm$$

- Measurement agrees with scaling.

$$A_{PV}({}^{N}_{Z}X) = \frac{-G_F Q^2}{4\pi\alpha\sqrt{2}} \left[Q_w^p + (\tfrac{N}{Z}) Q_W^n \right]$$

Aluminum background not expected to dominate systematic uncertainty.

Backgrounds

Neutrals: line of sight blocked

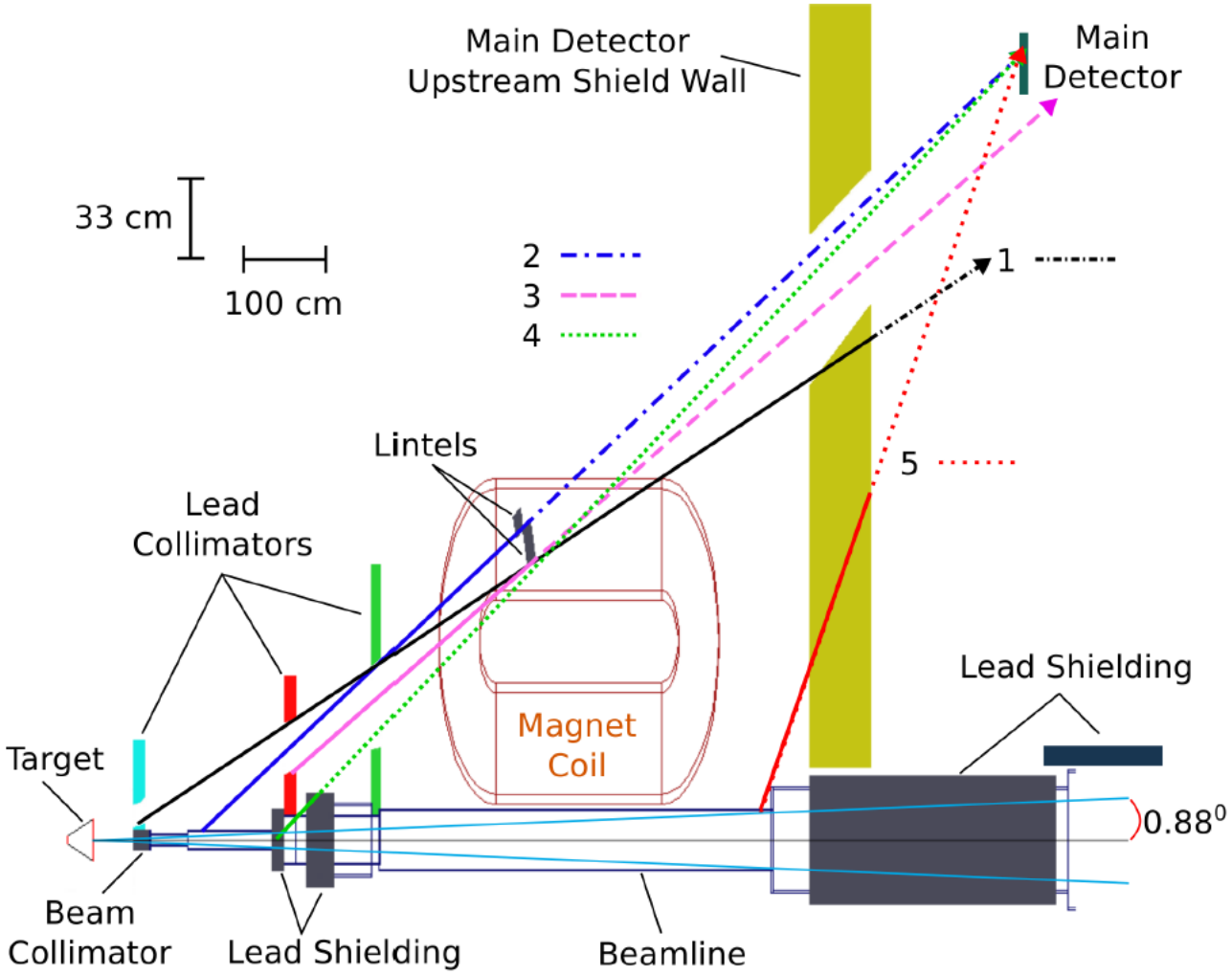

Removal of Background Asymmetries

- Background asymmetry observed even with defining collimator blocked
  - Correlated non-zero asymmetries observed in number of background detectors.
  - Found to be independent of QTor current (neutrals)
  - Strong dependence on raster size (helicity correlated beam halo interacting with tungsten collimator)

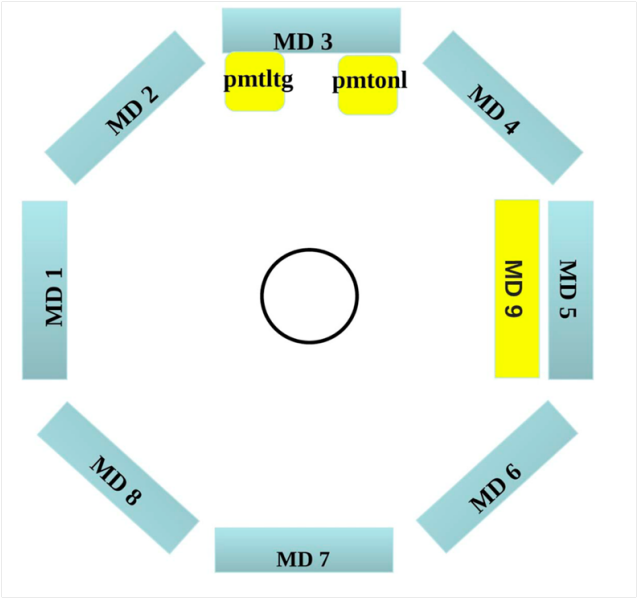

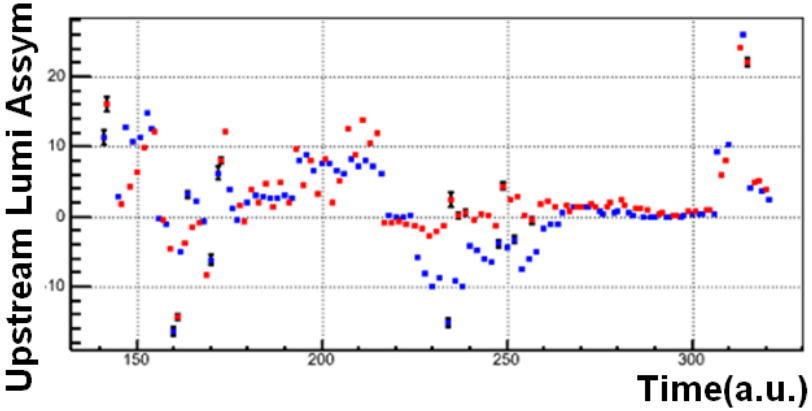

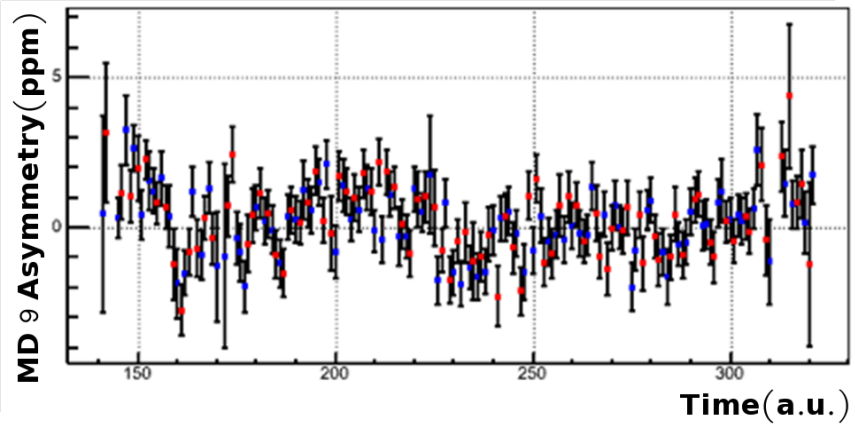

Removal of Background Asymmetries

- Strong correlation of neutral background with background detectors used to determine correction (11 ppb for Run 0)
- Background fraction determined by blocking octants in collimator
- Run 2 correction for beamline background nearly complete
- Run 1 correction more difficult: analysis ongoing

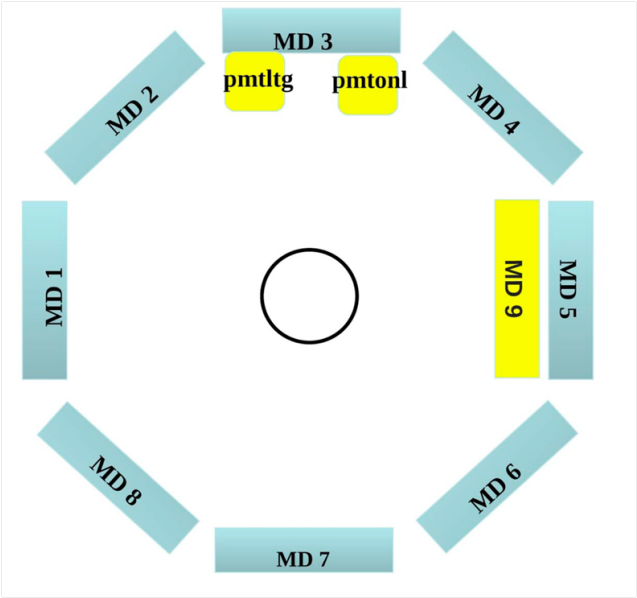

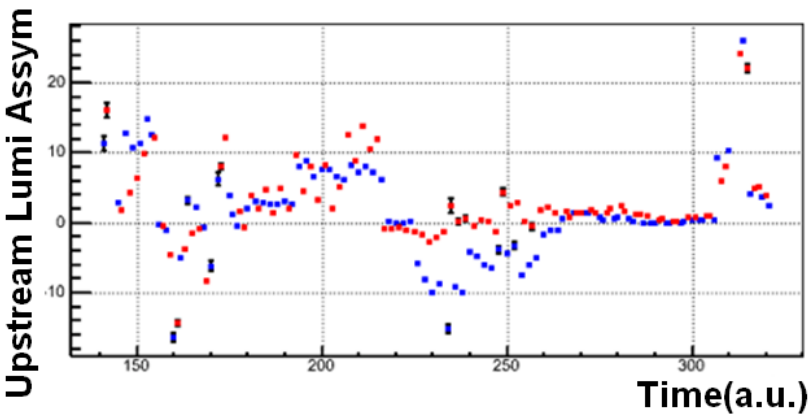

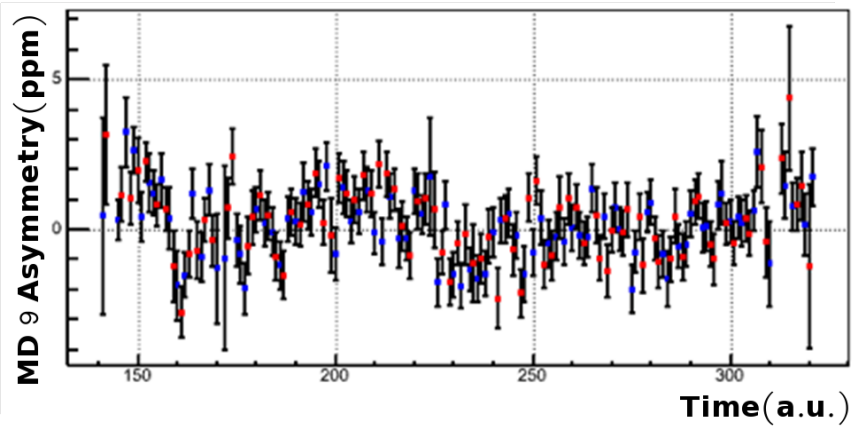

False Asymmetries: Helicity-Correlated Beam Properties

Electron beam properties that change in a way correlated to helicity reversal.

Three fold strategy for dealing with them

- Cancel –design experiment to cancel false asymmetries
  - Symmetric geometry to cancel sensitivity to beam trajectory
  - Slow helicity reversals: halfwave plate in laser, double wien flipper, number of passes through accelerator
- Minimize –careful setup of source and accelerator
  - Minimize position and angle differences from source laser
  - Set up accelerator for maximum adiabatic damping (beam trajectory differences reduced by $\sqrt{p_{Hall}/p_{source}}$)
  - Feed back on charge asymmetry
- Correct –measure and remove residual sensitivity to beam properties
  - Driven and natural beam motion to determine sensitivities

Cancel False Asymmetries with Slow Helicity Reversals

- Insertable half-wave plate (IHWP) in laser before cathode
- Reverses helicity w.r.t. Pockells cell HV.
- Cancels false asymmetries that don't change sign with laser polarization.
- Changed about every 8 hours.

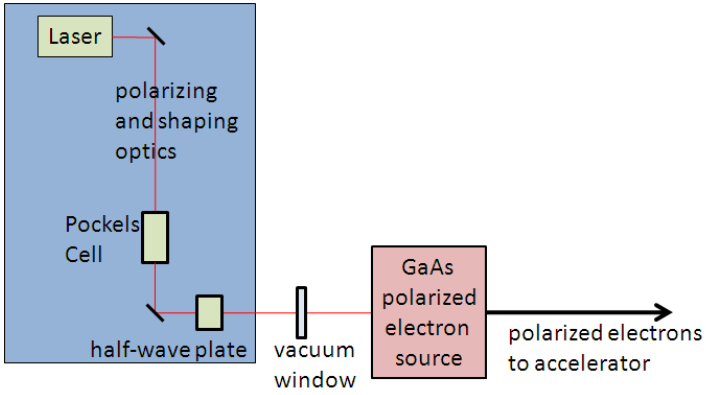

- Double Wien flips E-beam helicity.
- Cancel false asymmetries arising after IHWP that change sign with laser helicity (eg.birefringence in vacuum window).
- Changed 8 times during experiment.

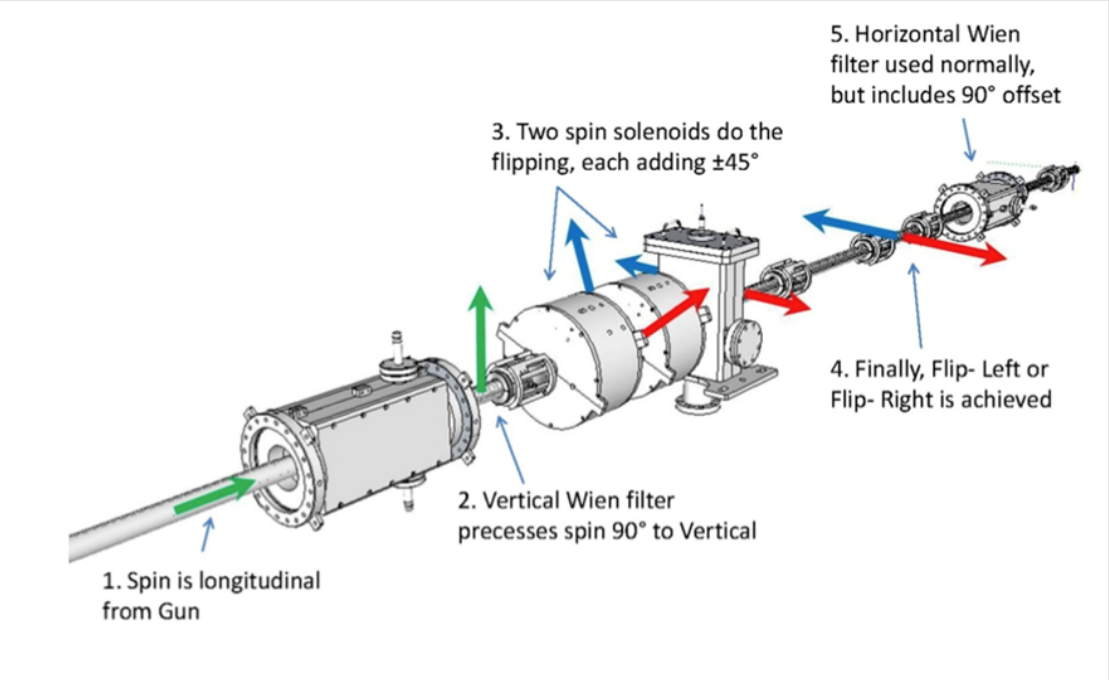

Cancel and Minimize: Beam Trajectory Differences

Run 2 Position Differences

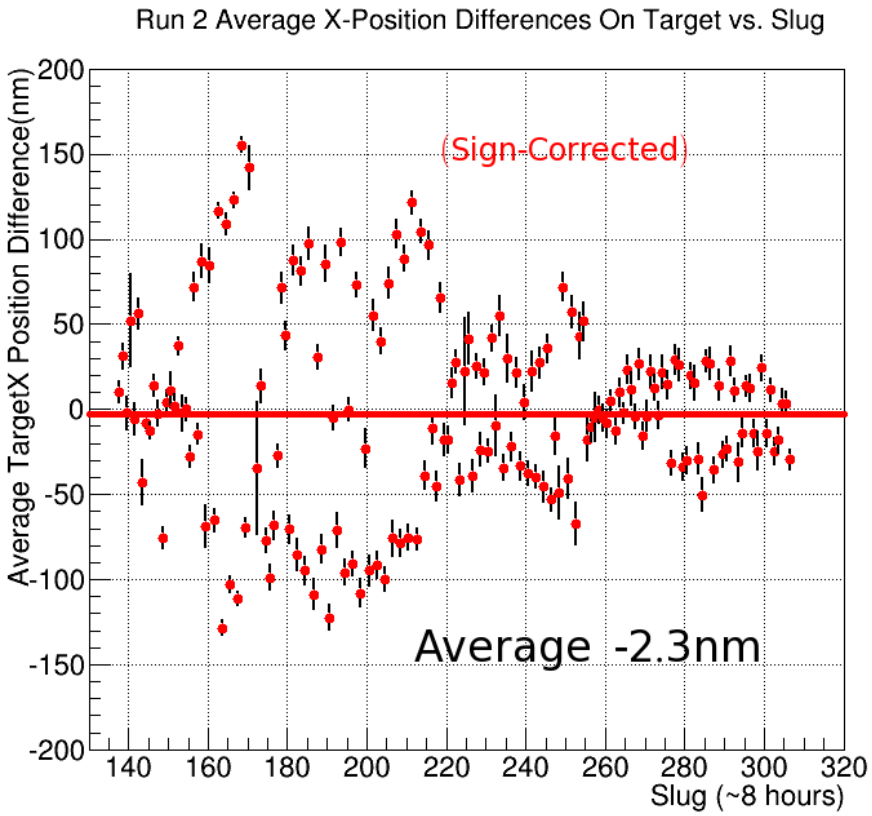

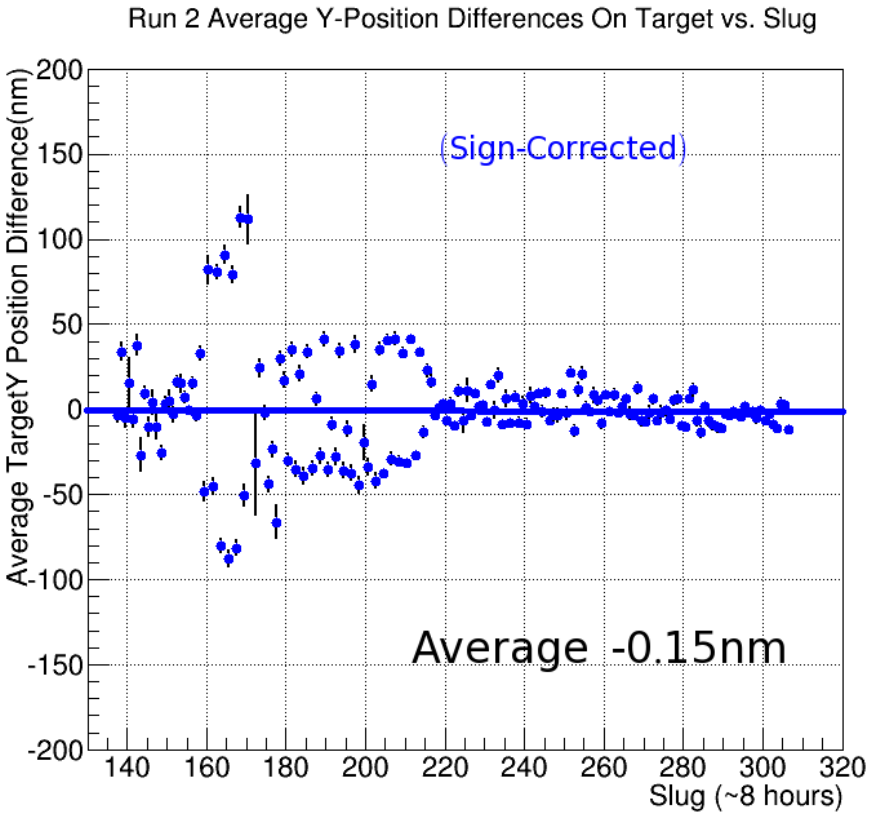

Minimize and Correct: Charge Asymmetry

Charge feedback on BPM in Hall C to source Pockels cell "PITA" voltage ensured $A_q \rightarrow 0$.

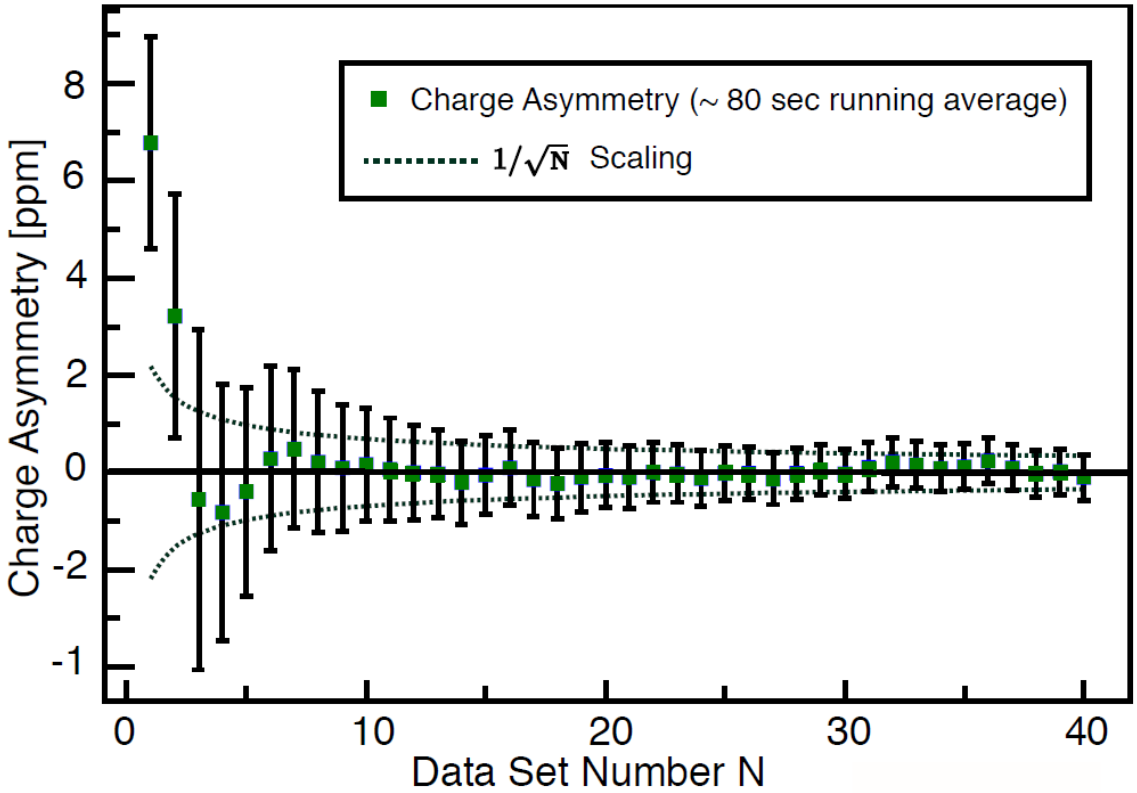

Normalize detectors to remove sensitivity to A_q.

Correct: Helicity Correlated Beam Properties

Correct using measured sensitivities $\frac{\partial A}{\partial x_i}$:

$$A_{PV} = A_{meas} - \sum \frac{\partial A}{\partial x_i} \Delta x_i, \qquad x_i = x, y, x', y', E$$

Slopes from Driven Beam Motion	Slopes from Natural Beam Motion
$\frac{\partial A}{\partial Coil_j} = \sum_{k=1}^{5} \frac{\partial A}{\partial x_k} \frac{\partial x_k}{\partial Coil_j}$	$\sum_{i=1}^{N} A_i (\Delta x_l)_i = \sum_{k=1}^{5} \frac{\partial A}{\partial x_k} \sum_i (\Delta x_l)_i (\Delta x_k)_i$
Express detector sensitivities to beam motion in driving air core magnet "coil" basis	Multivariable linear regression
Redundant driving modes allows cross check	Nulls sensitivity to beam motion by definition
Coils must span parameter space (x, x', y, y' and e)	Susceptible to error through correlations and monitor noise

Total correction for Run 2 $\sim 2ppb$ for both analyses.

Correct: Helicity Correlated Beam Properties

Correct using measured sensitivities $\frac{\partial A}{\partial x_i}$:

$$A_{PV} = A_{meas} - \sum \frac{\partial A}{\partial x_i} \Delta x_i, \qquad x_i = x, y, x', y', E$$

Slopes from Driven Beam Motion	Slopes from Natural Beam Motion
$\frac{\partial \mathbf{A}}{\partial \mathbf{Coil_j}} = \sum_{\mathbf{k=1}}^{\mathbf{5}} \frac{\partial \mathbf{A}}{\partial \mathbf{x_k}} \frac{\partial \mathbf{x_k}}{\partial \mathbf{Coil_j}}$	$\sum_{\mathbf{i=1}}^{\mathbf{N}} \mathbf{A_i}(\mathbf{\Delta x_l})_\mathbf{i} = \sum_{\mathbf{k=1}}^{\mathbf{5}} \frac{\partial \mathbf{A}}{\partial \mathbf{x_k}} \sum_\mathbf{i} (\mathbf{\Delta x_l})_\mathbf{i} (\mathbf{\Delta x_k})_\mathbf{i}$
Express detector sensitivities to beam motion in driving air core magnet "coil" basis	Multivariable linear regression
Redundant driving modes allows cross check	Nulls sensitivity to beam motion by definition
Coils must span parameter space (x, x', y, y' and e)	Susceptible to error through correlations and monitor noise

Total correction for Run 2 $\sim 2ppb$ for both analyses.

Correct: Helicity Correlated Beam Properties

Correct using measured sensitivities $\frac{\partial A}{\partial x_i}$:

$$A_{PV} = A_{meas} - \sum \frac{\partial A}{\partial x_i} \Delta x_i, \qquad x_i = x, y, x', y', E$$

Slopes from Driven Beam Motion	Slopes from Natural Beam Motion
$\frac{\partial \mathbf{A}}{\partial \mathbf{Coil_j}} = \sum_{\mathbf{k=1}}^{\mathbf{5}} \frac{\partial \mathbf{A}}{\partial \mathbf{x_k}} \frac{\partial \mathbf{x_k}}{\partial \mathbf{Coil_j}}$	$\sum_{\mathbf{i=1}}^{\mathbf{N}} \mathbf{A_i}(\mathbf{\Delta x_l})_\mathbf{i} = \sum_{\mathbf{k=1}}^{\mathbf{5}} \frac{\partial \mathbf{A}}{\partial \mathbf{x_k}} \sum_\mathbf{i} (\mathbf{\Delta x_l})_\mathbf{i} (\mathbf{\Delta x_k})_\mathbf{i}$
Express detector sensitivities to beam motion in driving air core magnet "coil" basis	Multivariable linear regression
Redundant driving modes allows cross check	Nulls sensitivity to beam motion by definition
Coils must span parameter space (x, x', y, y' and e)	Susceptible to error through correlations and monitor noise

Total correction for Run 2 $\sim 2ppb$ for both analyses.

Correct: Helicity Correlated Beam Properties

Correct using measured sensitivities $\frac{\partial A}{\partial x_i}$:

$$A_{PV} = A_{meas} - \sum \frac{\partial A}{\partial x_i} \Delta x_i, \qquad x_i = x, y, x', y', E$$

Slopes from Driven Beam Motion	Slopes from Natural Beam Motion
$\frac{\partial \mathbf{A}}{\partial \mathbf{Coil_j}} = \sum_{\mathbf{k=1}}^{\mathbf{5}} \frac{\partial \mathbf{A}}{\partial \mathbf{x_k}} \frac{\partial \mathbf{x_k}}{\partial \mathbf{Coil_j}}$	$\sum_{\mathbf{i=1}}^{\mathbf{N}} \mathbf{A_i}(\mathbf{\Delta x_l})_\mathbf{i} = \sum_{\mathbf{k=1}}^{\mathbf{5}} \frac{\partial \mathbf{A}}{\partial \mathbf{x_k}} \sum_\mathbf{i} (\mathbf{\Delta x_l})_\mathbf{i} (\mathbf{\Delta x_k})_\mathbf{i}$
Express detector sensitivities to beam motion in driving air core magnet "coil" basis	Multivariable linear regression
Redundant driving modes allows cross check	Nulls sensitivity to beam motion by definition
Coils must span parameter space (x, x', y, y' and e)	Susceptible to error through correlations and monitor noise

Total correction for Run 2 $\sim 2ppb$ for both analyses.

Corrections from Driven and Natural Beam Motion

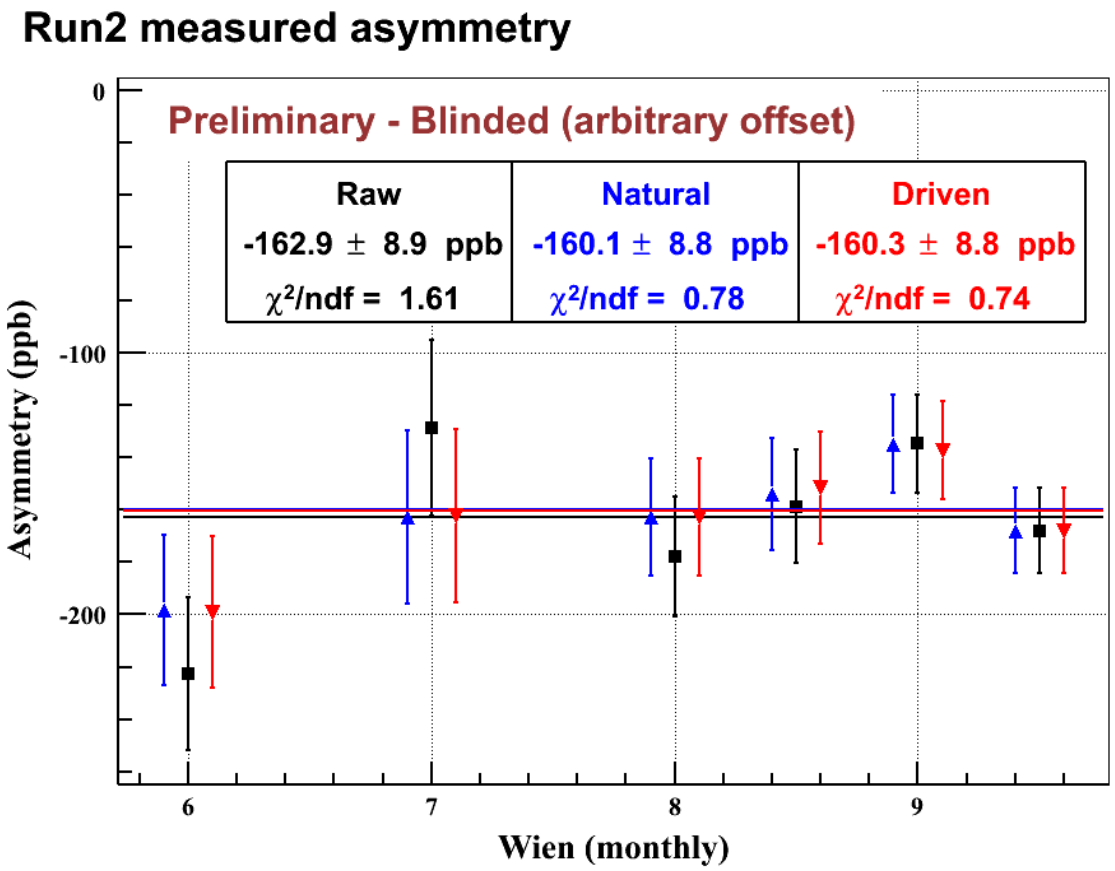

Looks good overall but subtleties in the analysis demand explanation.

Driven Motion aka Beam Modulation

- System design based on Hall A modeled and built by Mack and Nurruzzman
- Implemented during Qweak by Josh Hoskins
- Analysis passed to me after Qweak completion
- Subtleties currently being examined by Peng Zang (Syracuse)
- Drive beam well beyond its natural motion to find detector sensitivities to X, X', Y, Y' and Energy.
- 4 dipole magnets in Hall C arc: 2 dipoles to drive X, X' and 2 to drive Y, Y'. Energy vernier on accelerating RF cavity in south linac for E.
- Driven with a 125 Hz sinusoid.

The simplest model is five equations in five unknowns.
C=coil, D=detector, M=monitor

$$\frac{\partial D}{\partial C_k} = \sum_{i=1}^{5} \frac{\partial D}{\partial M_i} \frac{\partial M_i}{\partial C_k}$$

Beam Modulation

- Redundancy–drive the beam more than 5 ways (distortion modes).
- The beam should have only 5 DOF so each additional coil (distortion modes) will be a linear combination of X, X', Y, Y' and E.
- Extra information so must used χ^2 minimization to extract best solution from N coils leading to

$$\sum_{k=1}^{N} \frac{\partial D}{\partial C_k} \frac{\partial M_q}{\partial C_k} = \sum_{i=1}^{5} \frac{\partial D}{\partial M_i} \sum_{k=1}^{N} \left(\frac{\partial M_i}{\partial C_k} \frac{\partial M_q}{\partial C_k} \right)$$

- Redundancy gives internal consistency cross check and allows non-zero residual sensitivity.
- Absolutely necessary for precision PV experiments.
- 10-Coil redundancy inadvertantly implemented in Qweak.

Example Correction

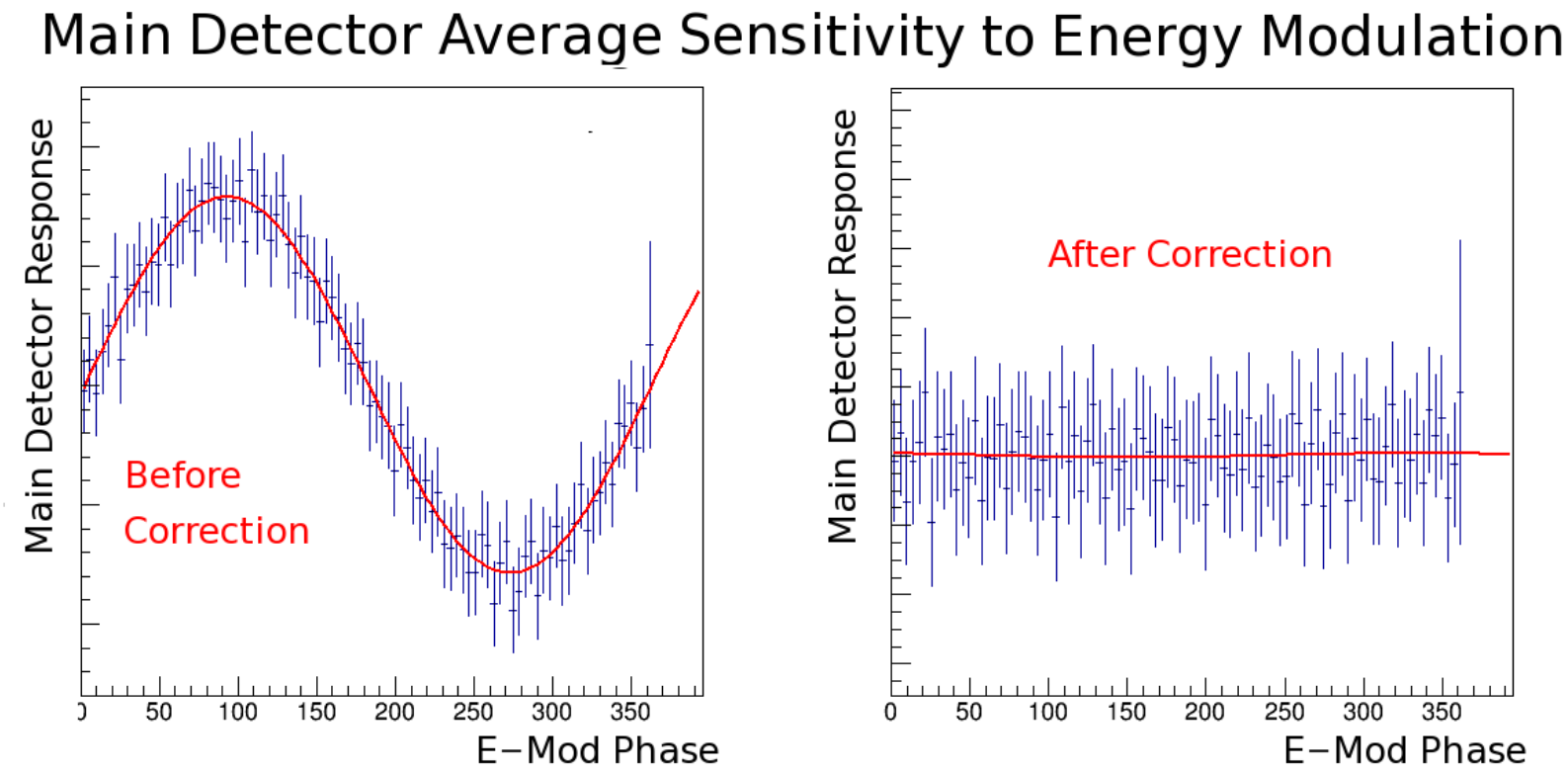

Corrections Compared across Coil Selections

Definitions Physics: correction averaged over HWP states
Null: 1/2 correction difference between HWP states

Run 1 Total correction by coil selection compared in units of ppb.

	10 Coil	Omit 0 (X1)	Omit 3 (X2)	Omit 5 (X1)	Omit 8 (X2)	Omit 3&5 (X1&2)	Omit 1,9 (Y1&2)
Physics	-16.9	-15.2	-54.8	-9.8	-16.6	-36.2	-16.8
Null	-22.3	-33.4	-109.9	-6.1	-21.3	-70.1	-22.0

Run 2 Total correction by coil selection compared in units of ppb.

	10 Coil	Omit 0 (X1)	Omit 3 (X2)	Omit 5 (X1)	Omit 8 (X2)	Omit 3&5 (X1&2)	Omit 1,9 (Y1&2)
Physics	-1.7	-3.4	-1.3	-1.4	-1.6	-1.8	-1.8
Null	+0.6	-22.0	-30.2	+7.5	+1.8	-13.4	+0.5

- Run 2 is much better behaved than Run 1
- Omitting coil 3 creates huge variations
- Physics is better than null so it appears affect cancels to some extent

Residual Correlations to BPM's

Go to production data (coils not modulating) to check correction results.

Main detector correlation to beam monitors after correction exacerbated by correction with slopes found omitting X2 modulation coils (in phase and out of phase)

MDall correlation slope to:	diff_targetX (ppb/nm)	diff_targetY (ppb/nm)	diff_targetXSlope (ppb/nrad)	diff_targetYSlope (ppb/nrad)	diff_energy ppb/ppb
10-Coil	-0.10 ± 0.15	-0.11 ± 0.29	-2.76 ± 5.71	-10.34 ± 9.93	1.36 ± 1.14
8-Coil(omit X1-coils)	-0.16 ± 0.15	-0.18 ± 0.29	-5.22 ± 5.71	-12.62 ± 9.93	1.54 ± 1.14
8-Coil(omit X2-coils)	-0.97 ± 0.15	-1.13 ± 0.29	-37.51 ± 5.79	-44.80 ± 10.05	1.76 ± 1.15

Conclusions for Beam Modulation Analysis

- We have an internal inconsistency in the beam modulation analysis.
- Physics results nearly consistent except when coil 3 omitted but omitting coil 3 is shown to be wrong from production data.
- So apply consistent 2 ppb correction to Run 2 and look more carefully at Run 1 to see if error can be reduced from 6 ppb spread.

Conclusions

- Qweak has completed the first direct measurement of the proton weak charge.
- Strict uncertainty limits allow Qweak to test key predictions of the Standard Model
- Electron beam polarimetry beat proposal goals due to the success of a new diamond electron detector and improvements in laser polarization measurement.
- Minimization, Cancellation and Correction of false asymmetries are critical component of PV experiments. Diagnostic and must be carefully designed and tested to ensure reliable results.
- Final results from Qweak will be published soon and are expected to test the Standard Model prediction of Q_W^p.
- Experience from Qweak will benefit the future parity program at Jefferson Lab

Thank You

Backup Slides

Mass Limits of new physics[1]: $\frac{\Lambda}{g} = \nu\sqrt{\frac{4\sqrt{5}}{\Delta Q_w^p}}$

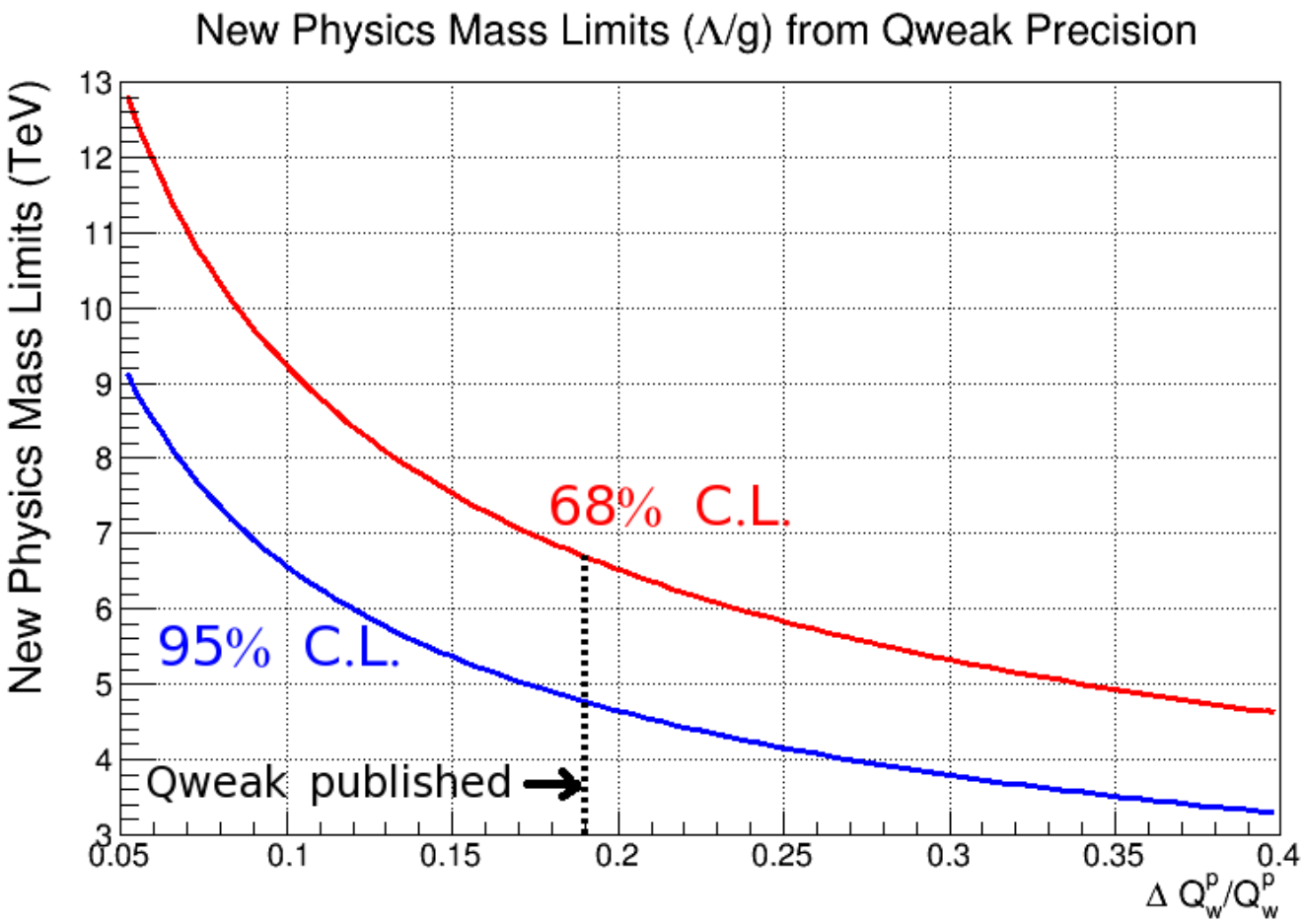

[1] *Weak Polarized Electron Scattering*, Erler et al (http://arxiv.org/abs/1401.6199)

Correction from γZ Box Diagram

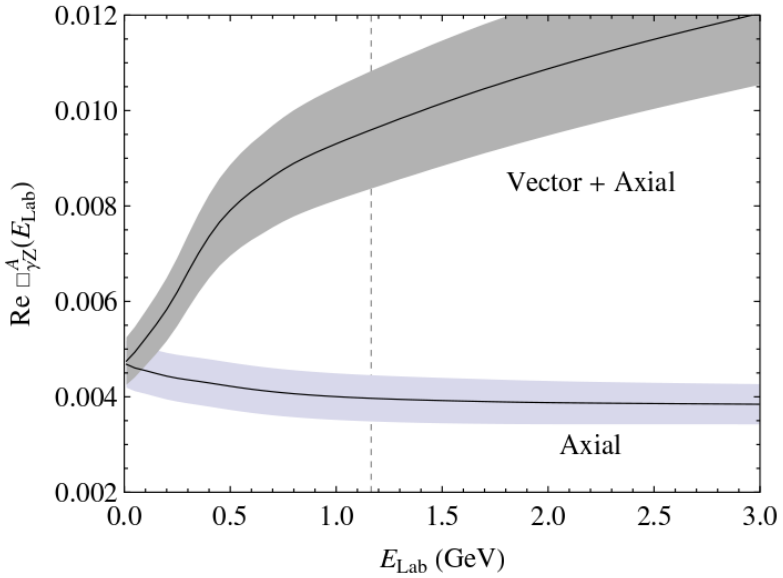

Table: Correction to Standard Model $Q_W^p = 0.0713(8)$ from axial proton ($\mathcal{R}e\Box^A_{\gamma Z}$) and vector proton ($\mathcal{R}e\Box^V_{\gamma Z}$) components of $\mathcal{R}e\Box_{\gamma Z}$ evaluated at Qweak kinematics $Q^2 = 1.165\ GeV$.

$\mathcal{R}e\Box^V_{\gamma Z}$		
	Sibirtsev *et al.* (2010)	$0.0047^{+0.0011}_{-0.0004}$
	Carlson and Rislow (2011)	0.0057 ± 0.0009
	Gorchtein *et al.* (2011)	0.0054 ± 0.0020
	Hall *et al.* (2013)	0.00557 ± 0.00036
$\mathcal{R}e\Box^A_{\gamma Z}$		
	Blunden *et al.* (2011)	$0.0037^{+0.0011}_{-0.0004}$
	Carlson and Rislow (2013)	0.0040 ± 0.0005

Electron Beam Polarization

Dedicated study for comparison of Compton and Moller at low current to verify validity of Moller results at high current.

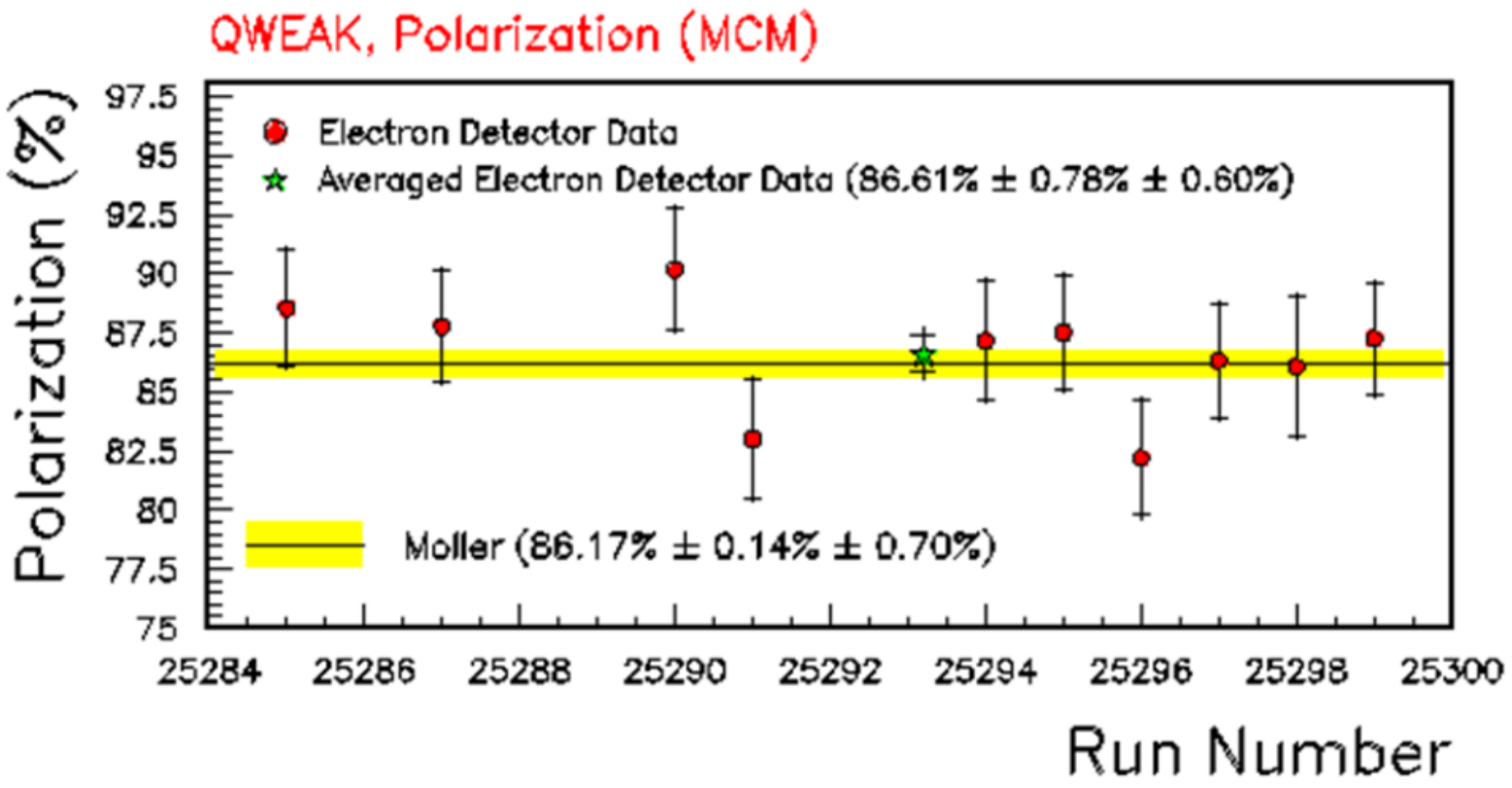

- The cross section of Compton scattering is different for right and left circularly polarized photons on polarized electrons.

$$\sigma_{R_e R_\gamma} = \sigma_{L_e L_\gamma} > \sigma_{L_e R_\gamma} = \sigma_{R_e L_\gamma}$$

$$A_{Comp} = \frac{\sigma_+ - \sigma_-}{\sigma_+ + \sigma_-}$$

$$\boxed{A_{meas} = P_\gamma P_e A_{Compton}}$$

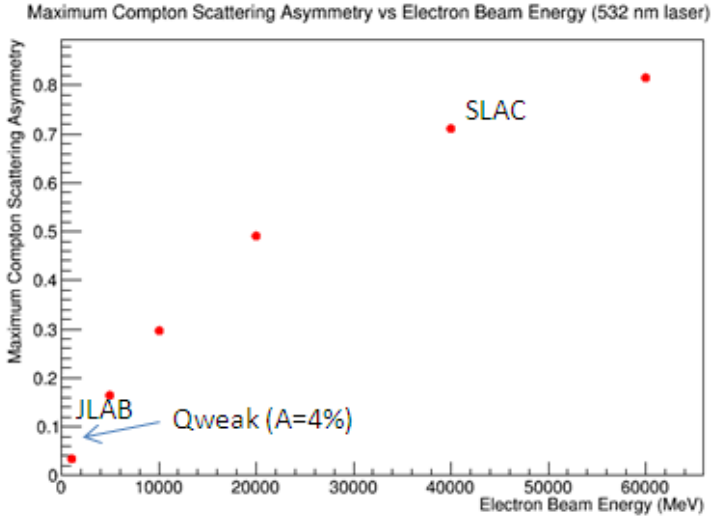

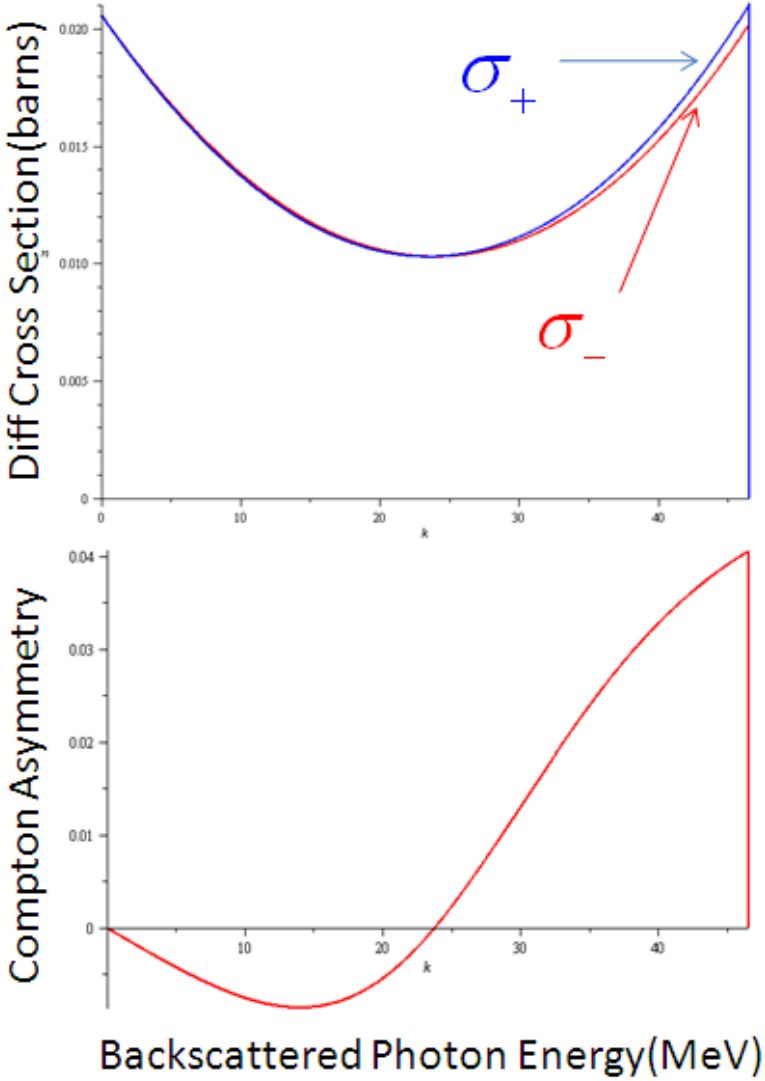

Photon Target Considerations

- 10 W Coherent Verdi laser locked to Fabry-Perot optical cavity with feedback on wavelength.
- Manufacturer stated line width <5MHz rms over 50ms. Not obvious that it was possible to lock to an optical cavity with a linewidth ~100-300kHz.
- Measurements on a similar laser (different feedback hardware) showed intrinsic linewidth ~150kHz.
- Stable lock with cavity of gain>200 and linewidth ~250kHz.
- Lock hard to maintain on higher finesse cavity with linewidth ~95 kHz. Unclear whether it was electronics or linewidth that was limiting factor.

Cavity Specs:

Length	85cm
Mirror Ref	0.995
Mirror Tran	0.005
Mirror Loss	>50ppm

Locking the Optical Cavity with PDH Method

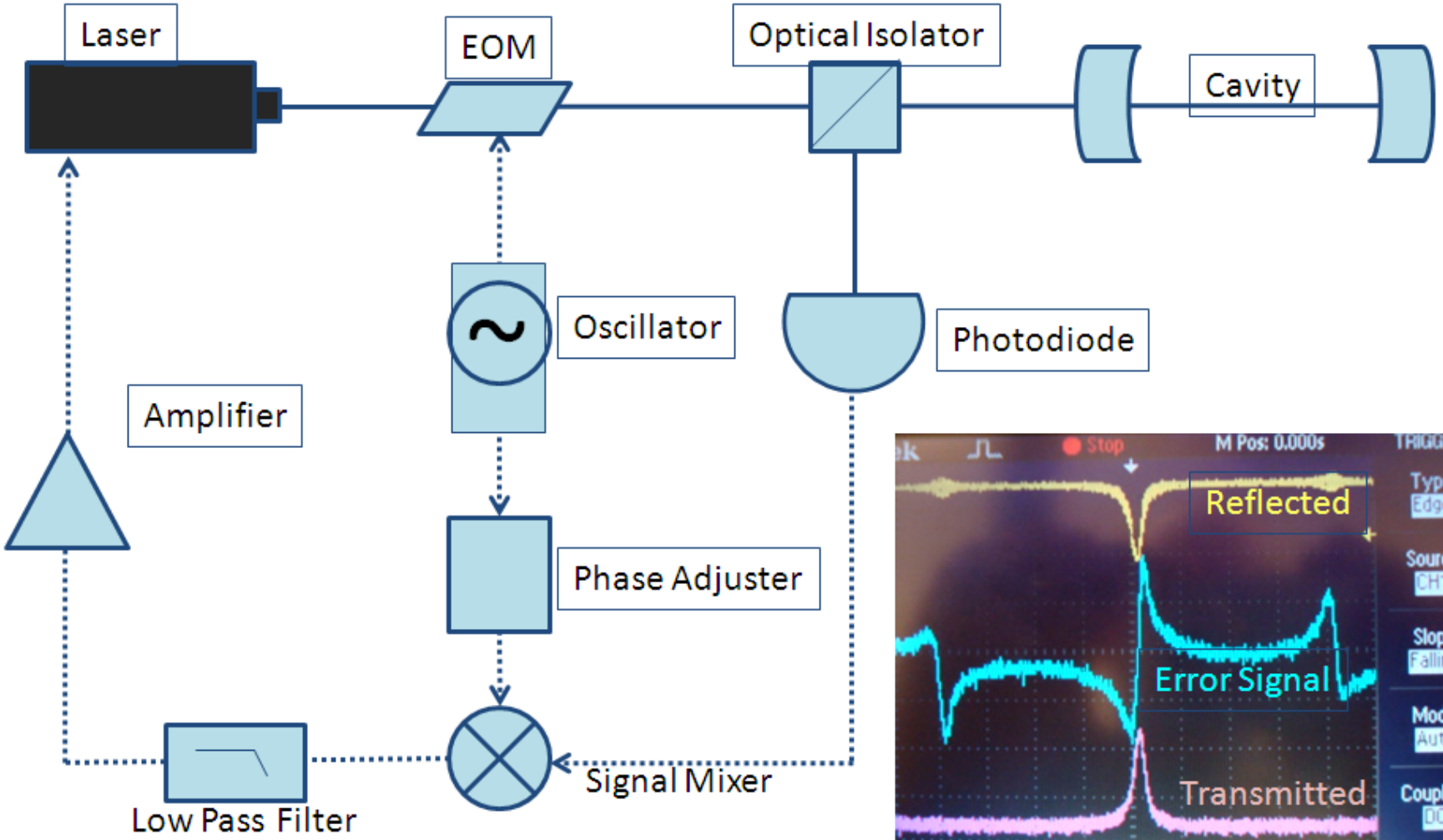

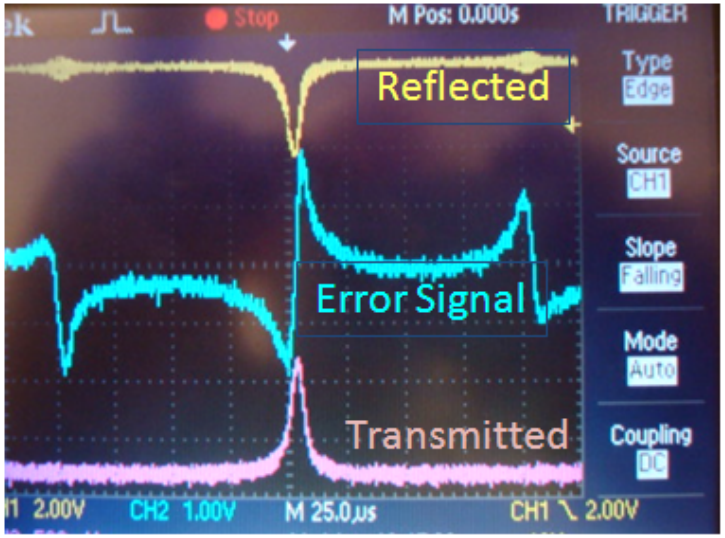

Photon Target for Compton Polarimeter

- Toptica Digital Electronics for cavity lock
- LabVIEW based monitoring and remote control of laser position.alignment and power
- Remote monitoring and control of laser polarization and helicity
- Communication with Jlab's EPICS program for continuous data logging of key parameters

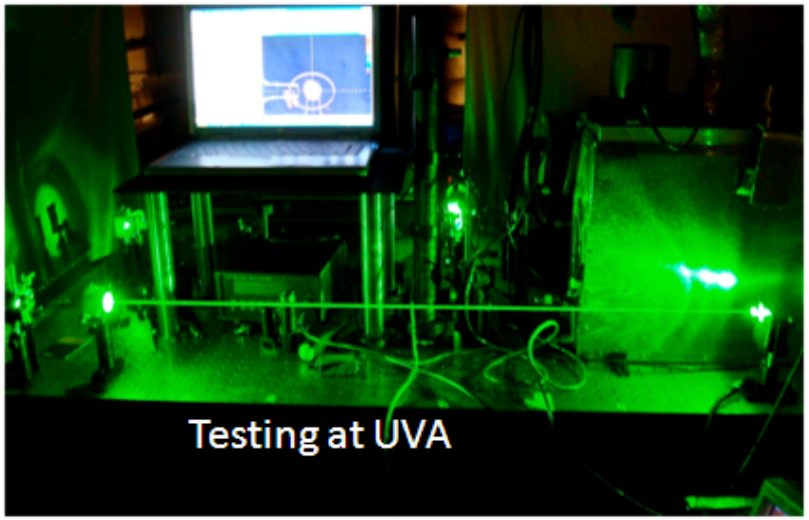

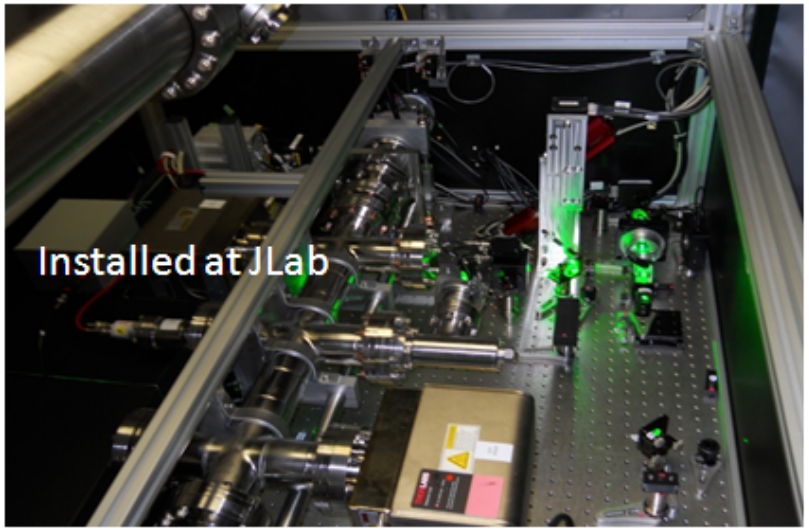

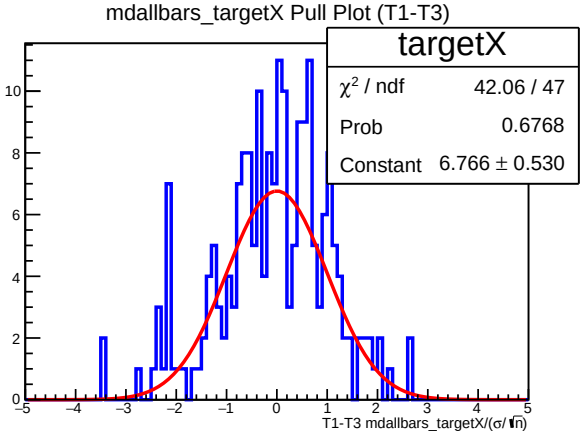

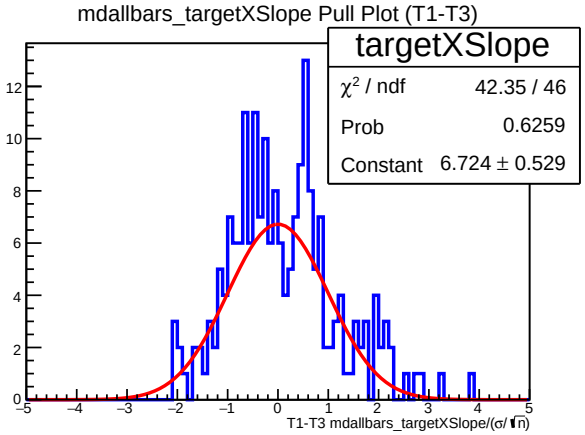

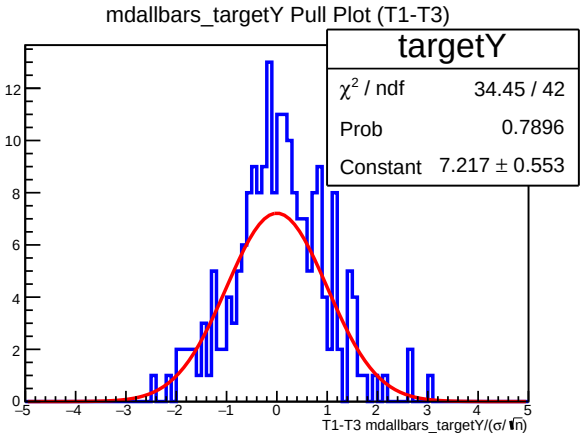

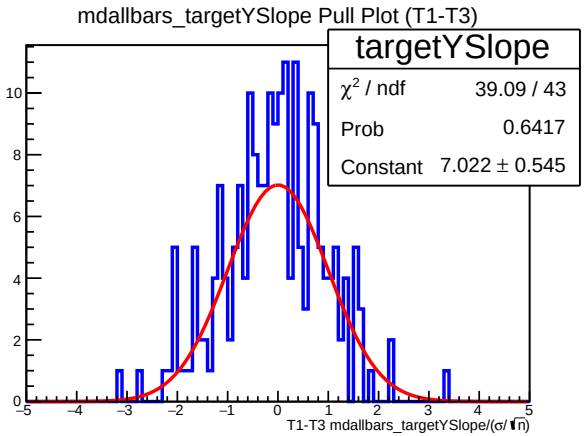

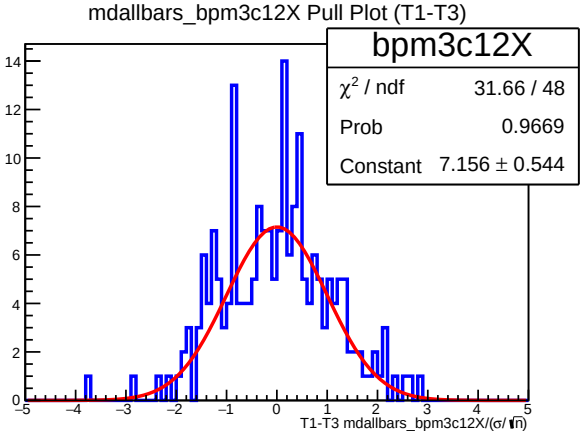

Tertile 1 - Tertile 3 mdallbars correction slope pull plots

$$\frac{\text{(T1.mdallbars_monitor-T3.mdallbars_monitor)}}{\text{Error}}$$

Average is over slugs and error is RMS/$\sqrt{n}$ for that slug

Evacuated LH2 Target Yields (Q-weak Run 1)

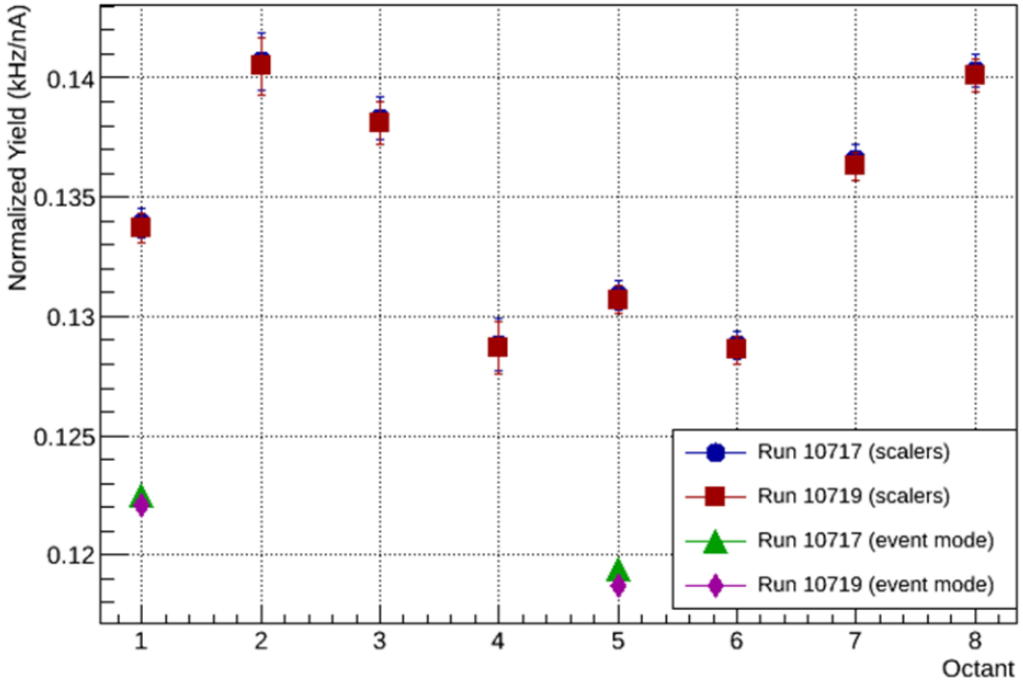

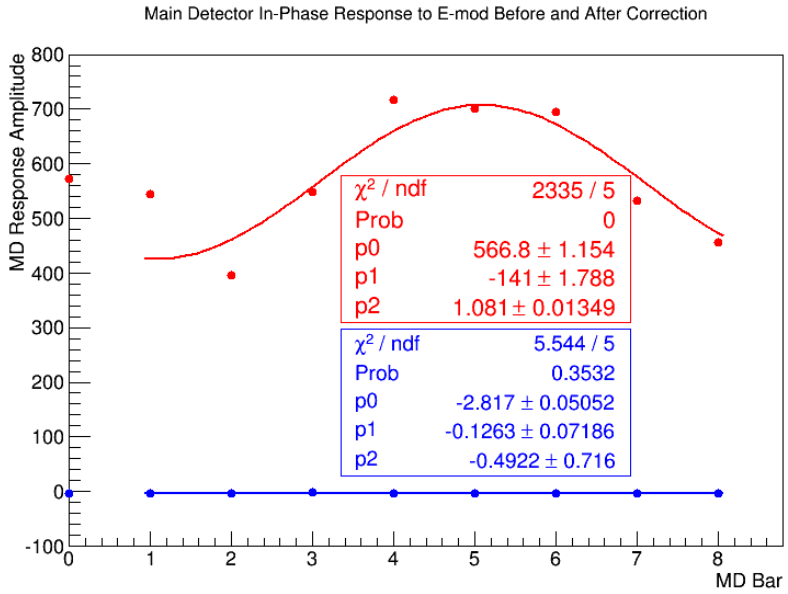

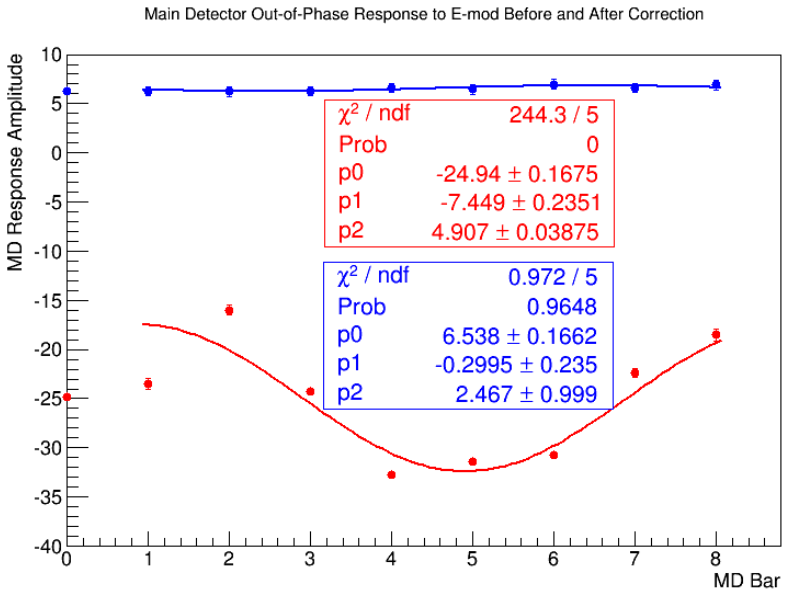

Transverse Rate Profile

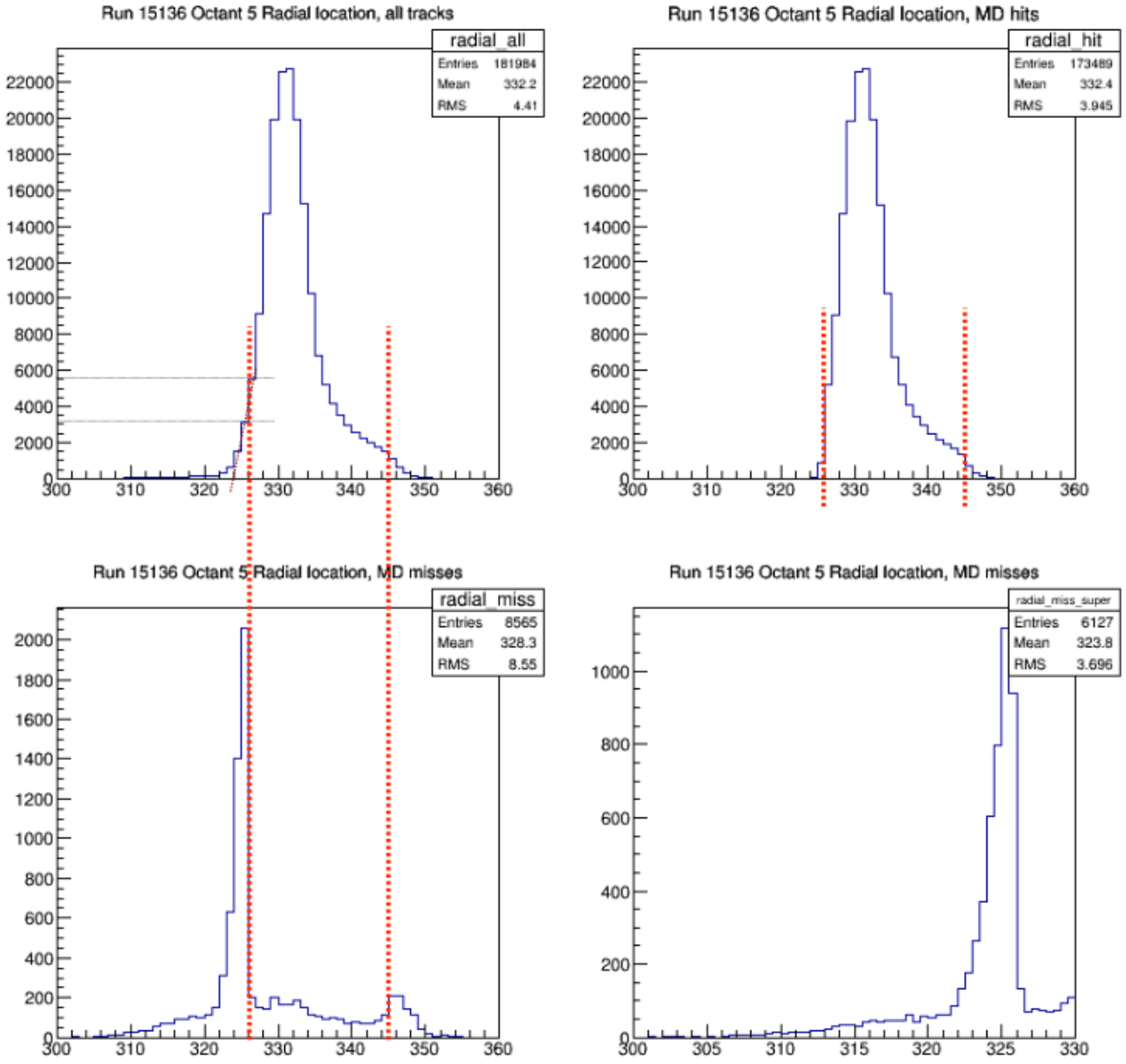

Figures by D. Armstrong, WM logbook elog:90

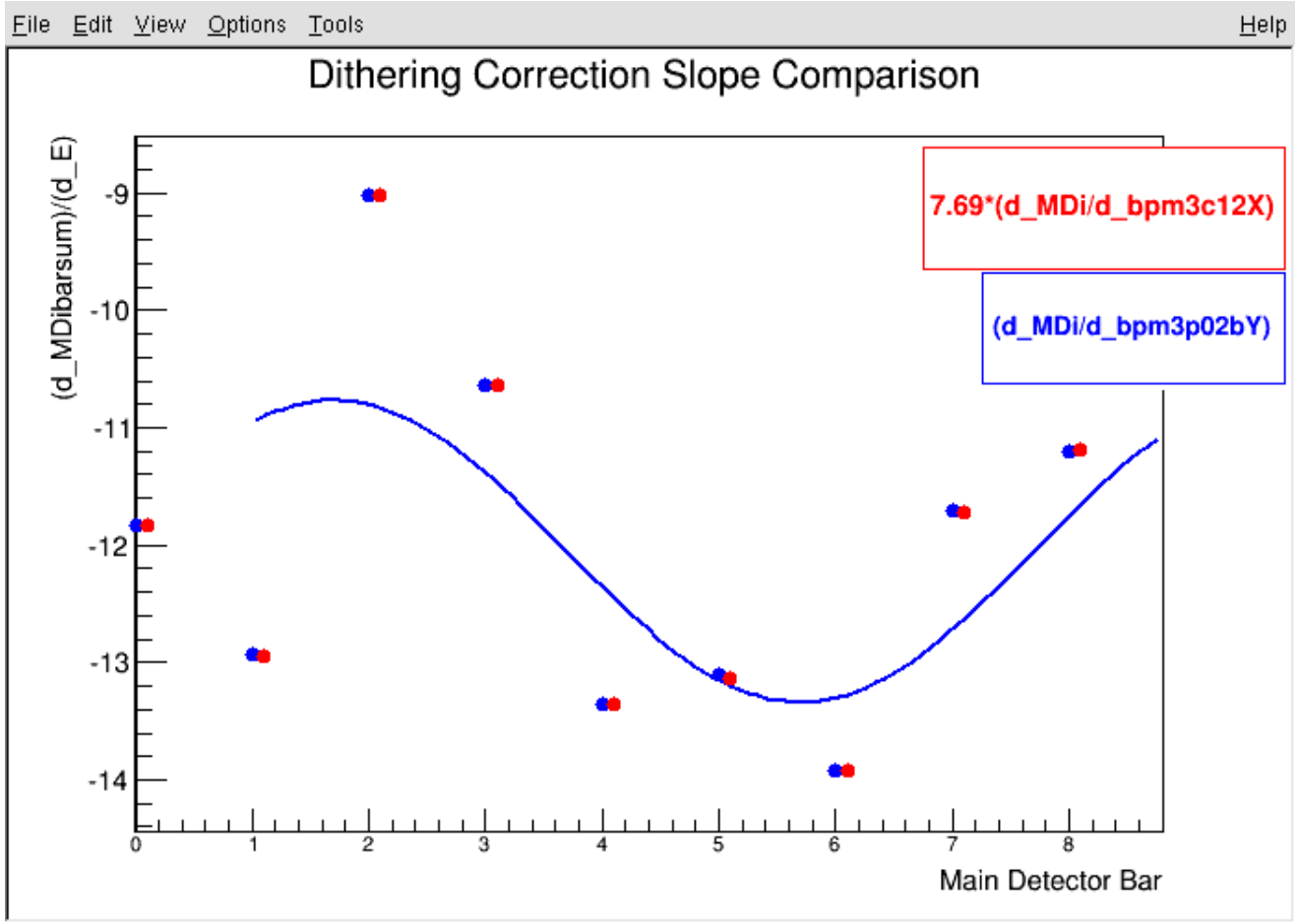
File Edit View Options Tools
Help
Dithering Correction Slope Comparison
(d_MDibarsum)/(d_E)
-9
-10
-11
-12
-13
-14
0
1
2
3
4
5
6
7
8
Main Detector Bar
7.69*(d_MDi/d_bpm3c12X)
(d_MDi/d_bpm3p02bY)

Measuring Intracavity Degree of Circular Polarization (DOCP)

- Measure laser polarization in exit line
- Measure Transfer Matrix (TM) to determine intracavity polarization from exit line measurement
- Accurately measure identical polarization states in the cavity and exit line regions to find TM.
- Problem! The TM unstable when
  →tightened flanges near windows
  →pulled vacuum and baked system

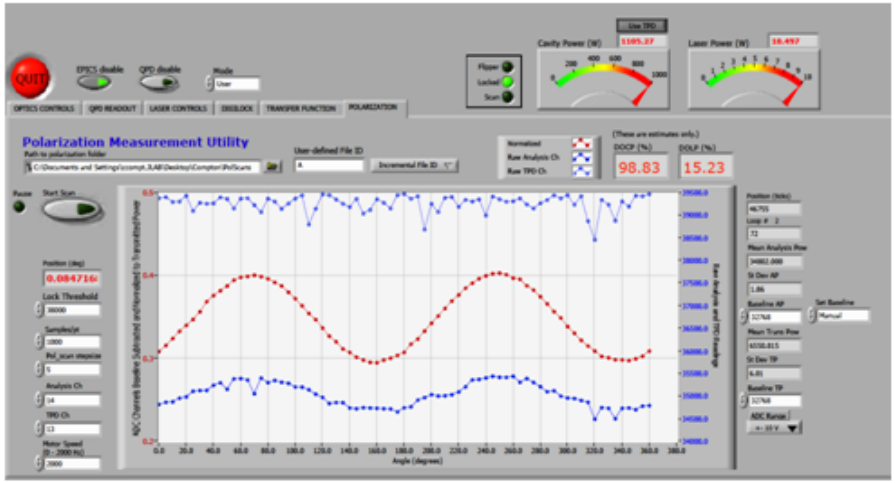

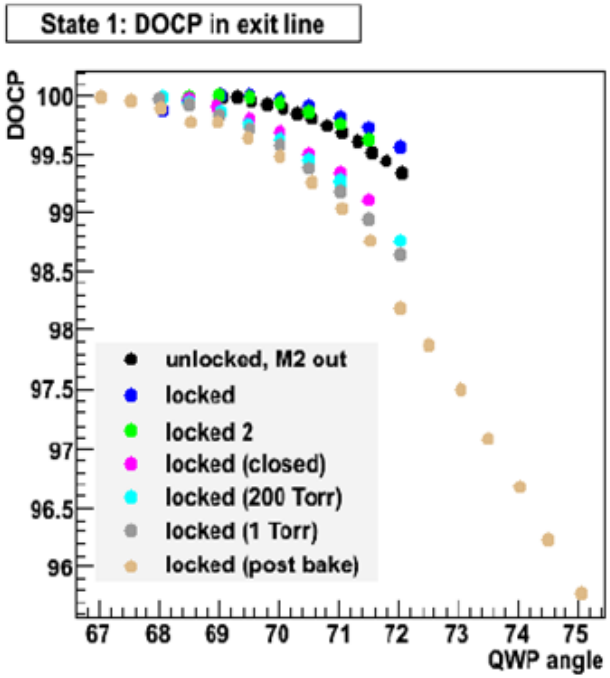

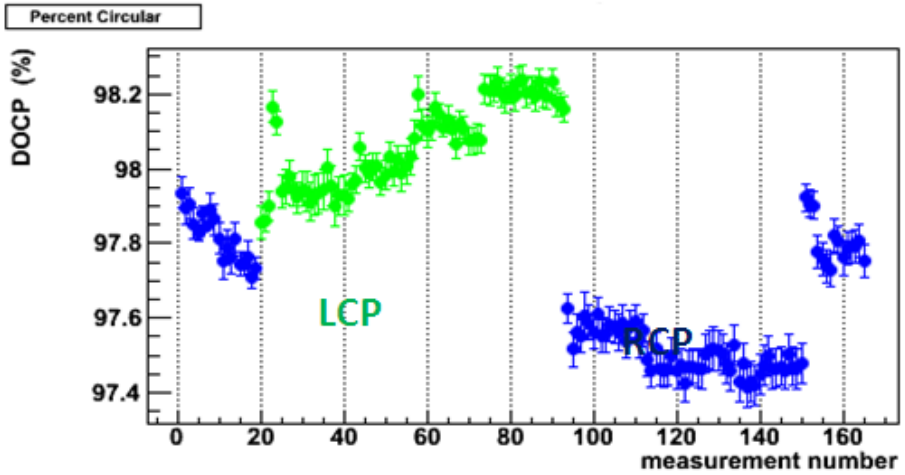

Correlation of DOCP to Reflected Light

- "Reflection leakage" anti-correlated to DOCP
- Convinced ourselves this was a fundamental relationship and decided to minimize the reflection leakage to maximize DOCP
- Later found a publication detailing the use of this technique for remote control of laser polarization.
- Added an extra HWP to the hardware to allow the setup of any arbitrary polarization state

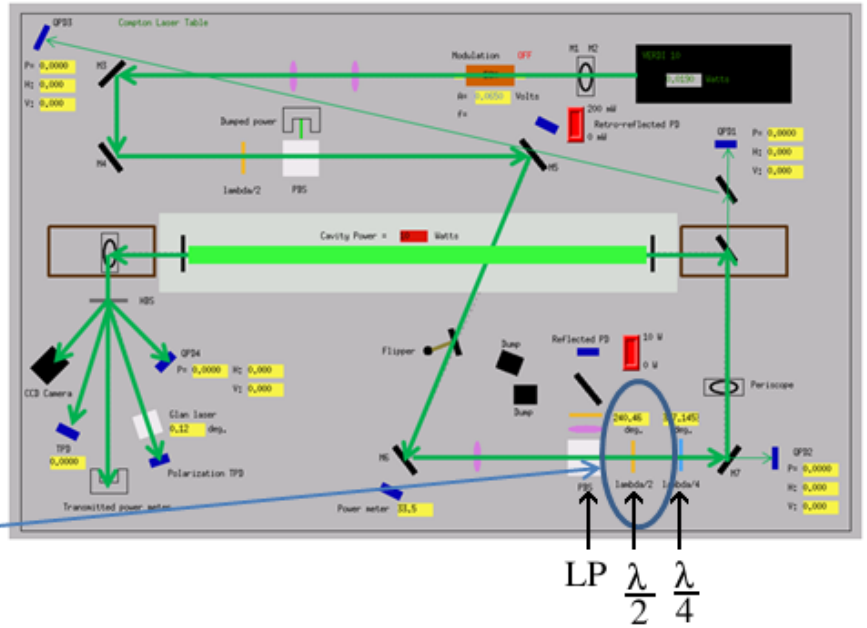

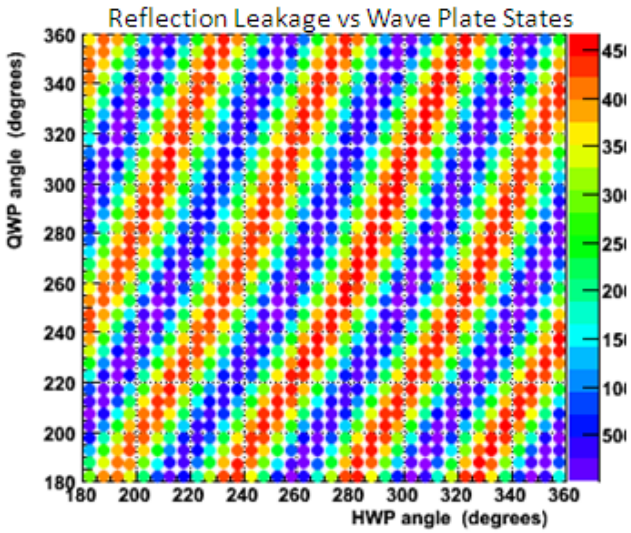

Optical reversibility theorems for polarization: application to remote control of polarization

N. Vansteenkiste, P. Vignolo,* and A. Aspect

Institut d'Optique, Unité Associée au Centre National de la Recherche Scientifique No. 14, Centre Scientifique d'Orsay, Bâtiment 503, BP 147, 91403 Orsay Cedex, France

Received March 11, 1993; accepted April 20, 1993

Using Jones's formalism, we prove three optical reversibility theorems that relate the polarization ellipticity at the output of an optical system to the polarization of the retroreflected light at the input. We describe how these theorems can be used to measure the ellipticity of a polarization remotely and thus to control it remotely. As an example, we use this method to create a linear or a circular polarization after a total internal reflection inside a prism, and the impurity of polarization is found to be better than 10^{-3}. Finally we describe the use of this remote control to create polarization configurations that are useful for laser cooling of atoms.

Sanity Check Using Electron Detector

- Varied laser polarization according to the model around the peak 100% DOCP position under stable electron beam conditions
- Results from preliminary electron detector asymmetries verify that we were indeed running on a peak DOCP
- We can at least say that the model correctly determines position of a maximum of DOCP

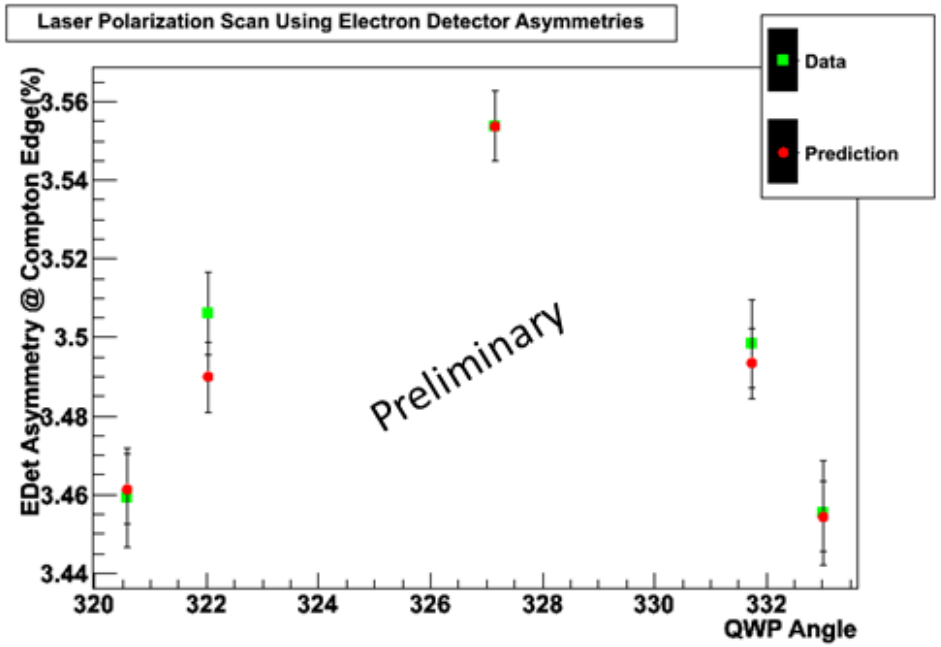

BPM Response Phase Slip Traced to FFB Activity (X)

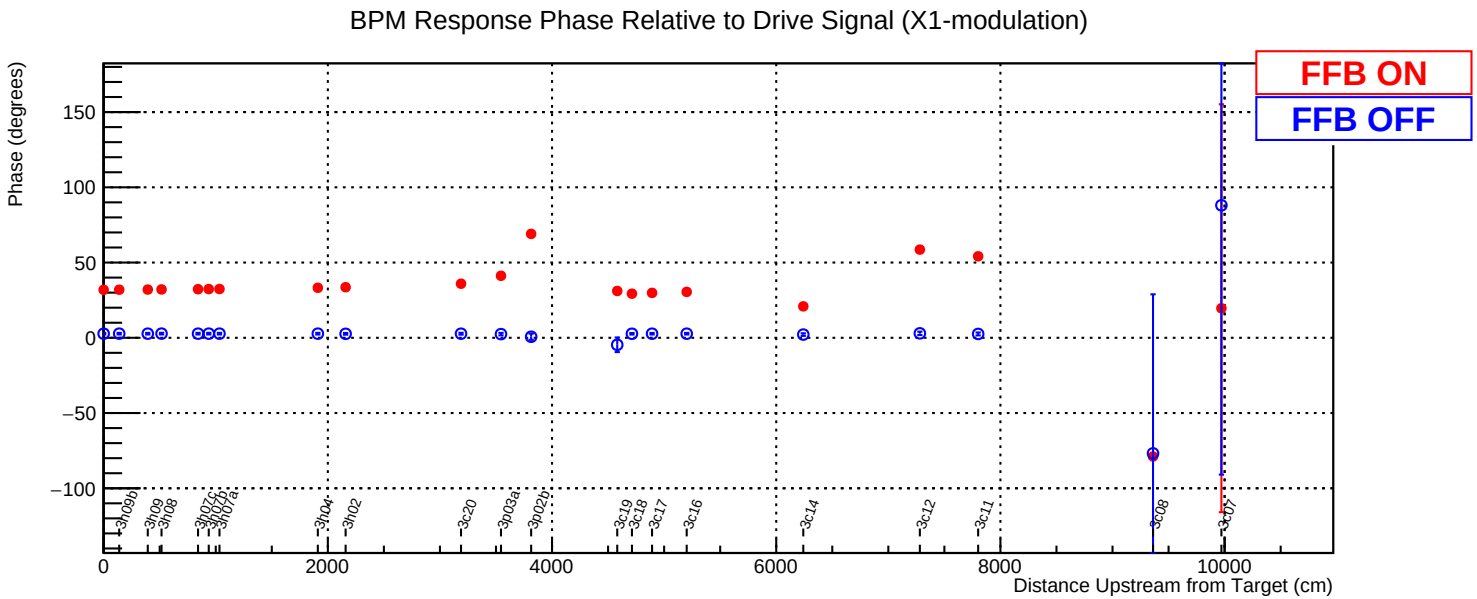

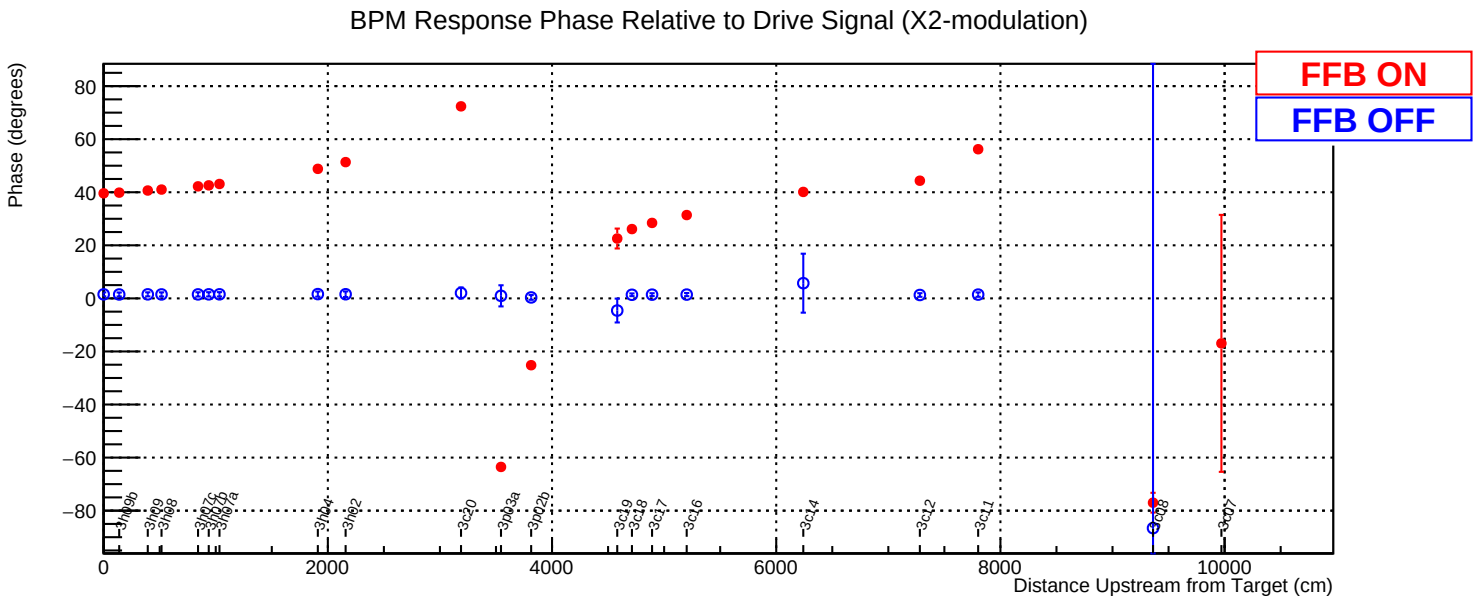

BPM Response Phase Slip Traced to FFB Activity (Y)

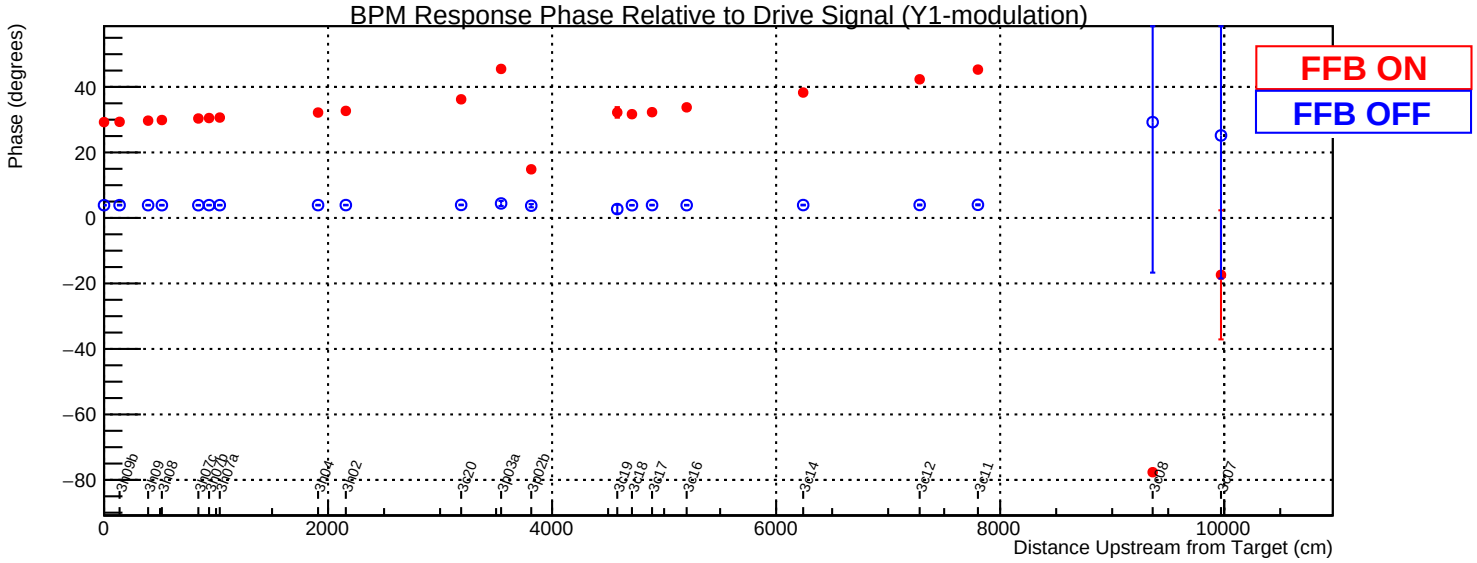

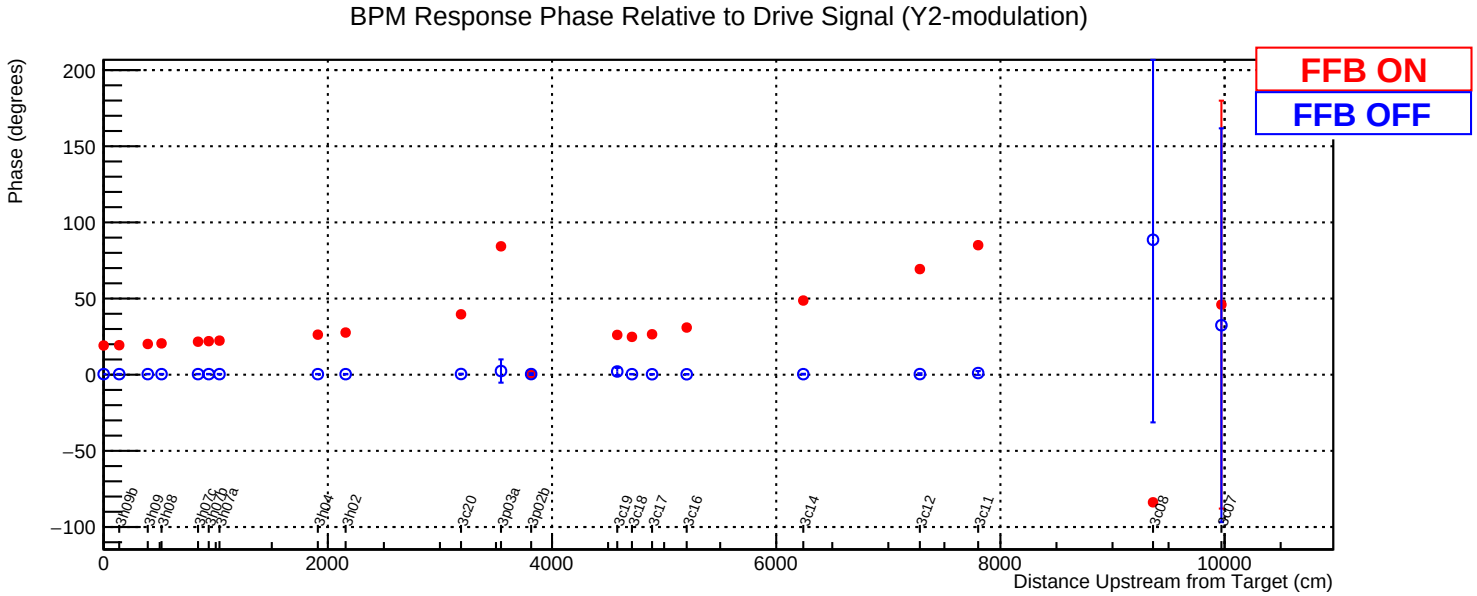

BPM Amplitude Response with FFB On and Off (X)

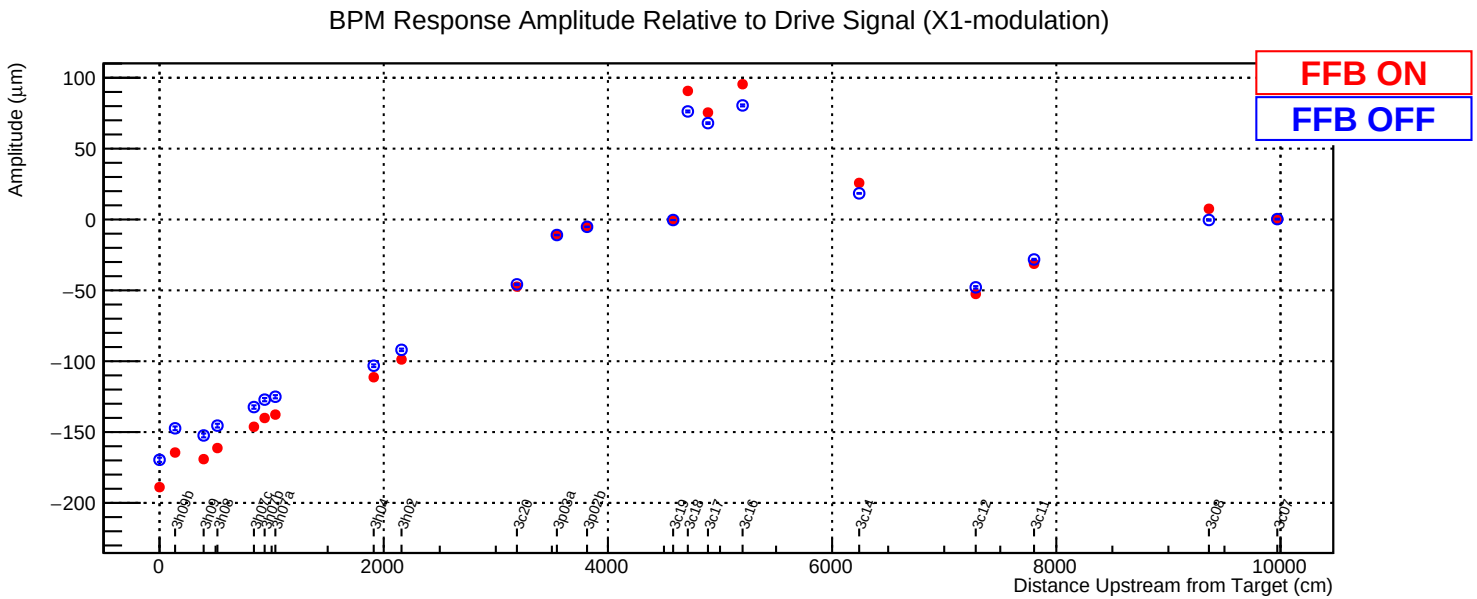

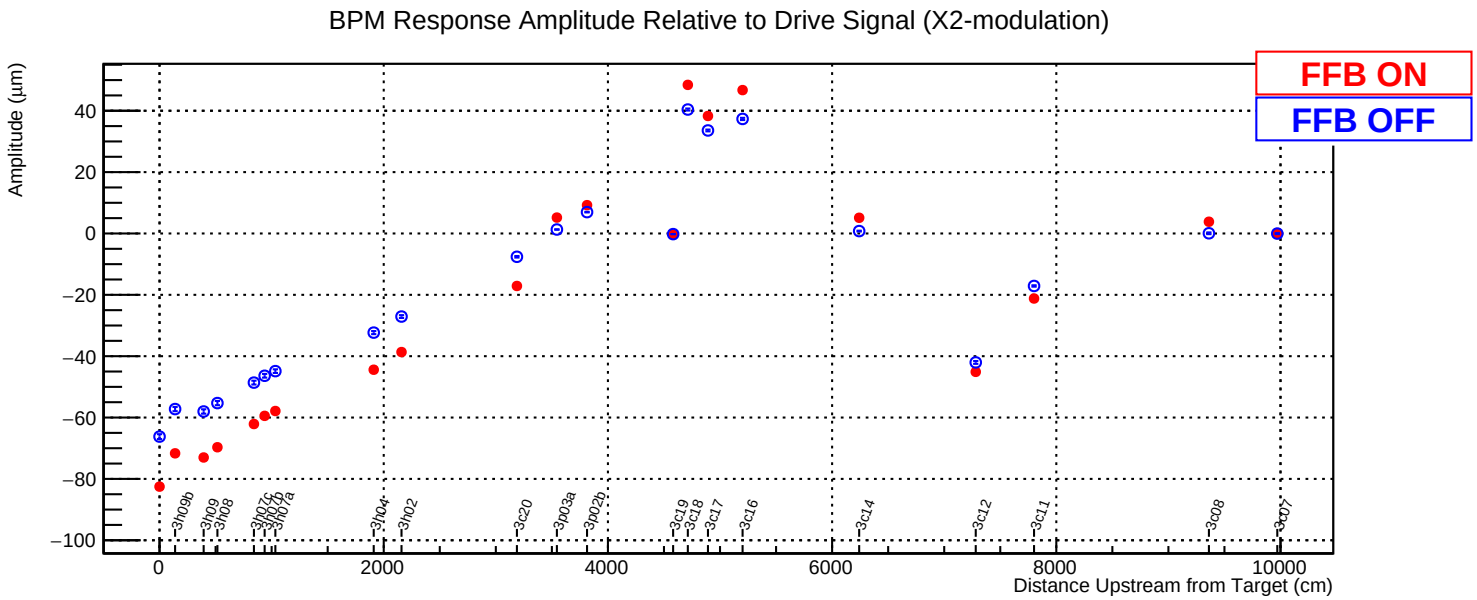

BPM Amplitude Response with FFB On and Off (Y)

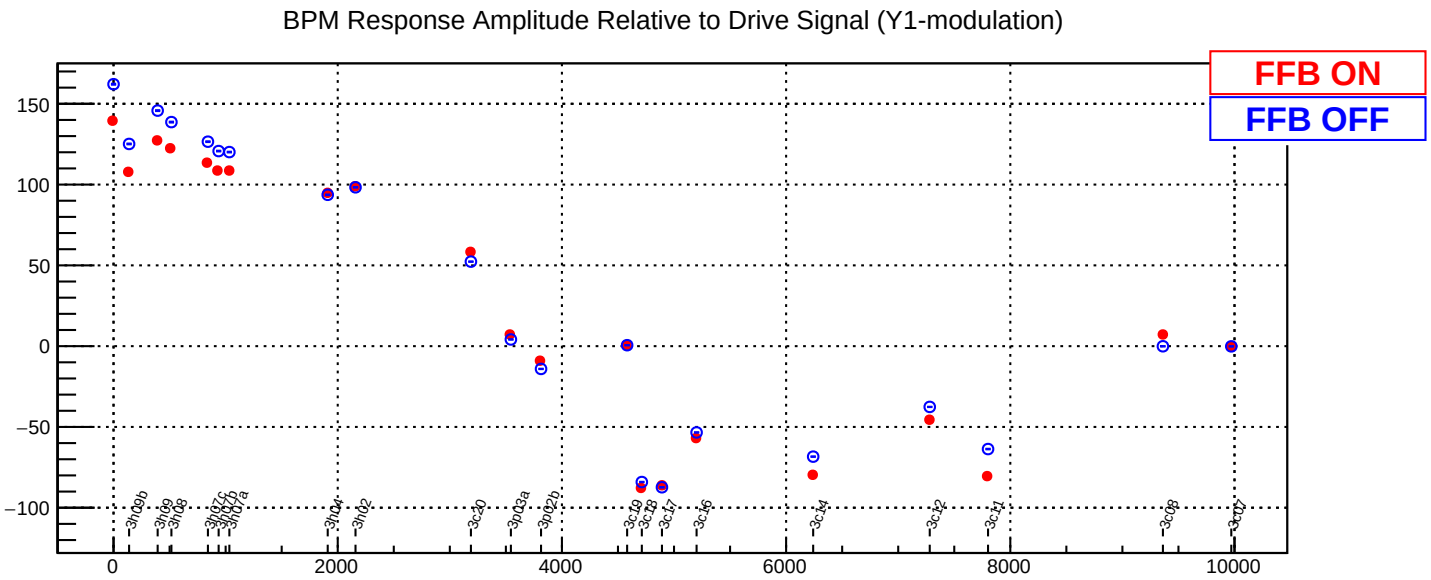

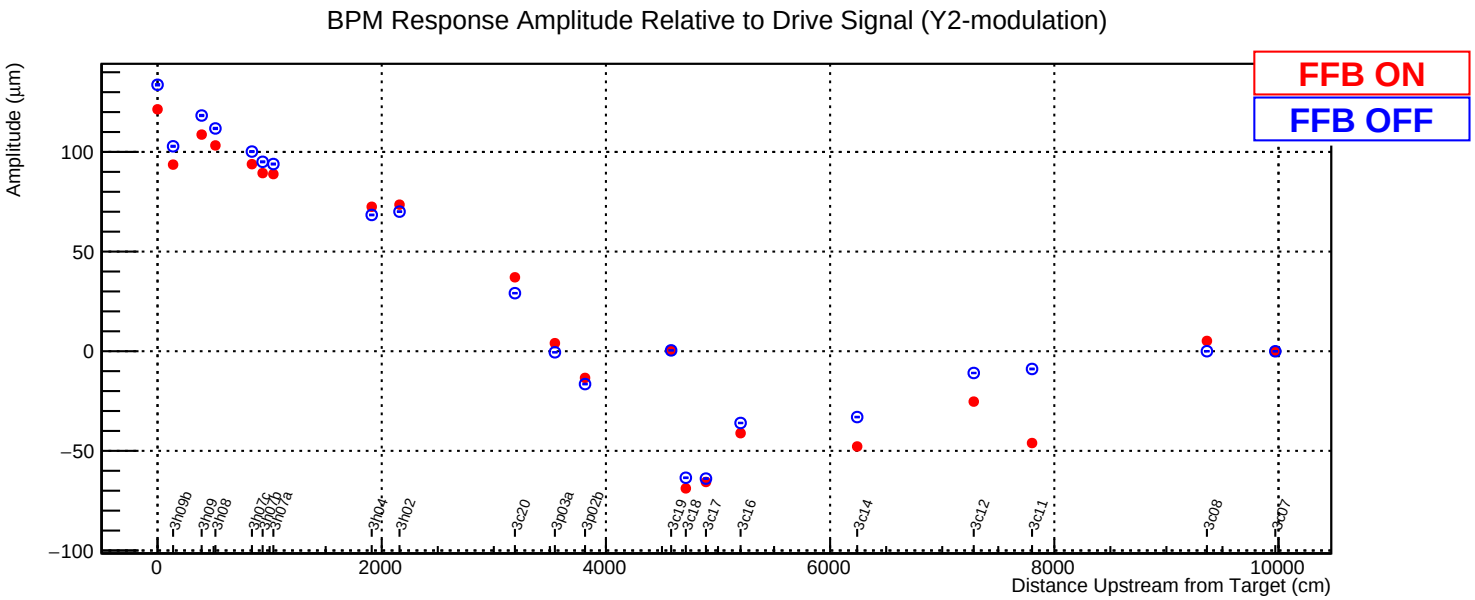

Beam Modulation

Out of caution (paranoia) FFB was left active even during modulation.

Modulated with only 5 modes but ended up with 10 using FFB responses.

FFB delayed response but stable and at same frequency 125 Hz

Analysis implements 10-coil redundancy:
–5 BPM responses in-phase with modulation coils (sine amplitudes)
–5 BPM responses out-of-phase with modulation coils (cosine amplitudes associated with FFB)

Independent simultaneous modulation modes 1/4 cycle out of phase.

Important to realize that this is a legitimate analysis decision.

Response Amplitudes to Modulation Modes

X1 Mode | Y1 Mode | E Mode | X2 Mode | Y2 Mode

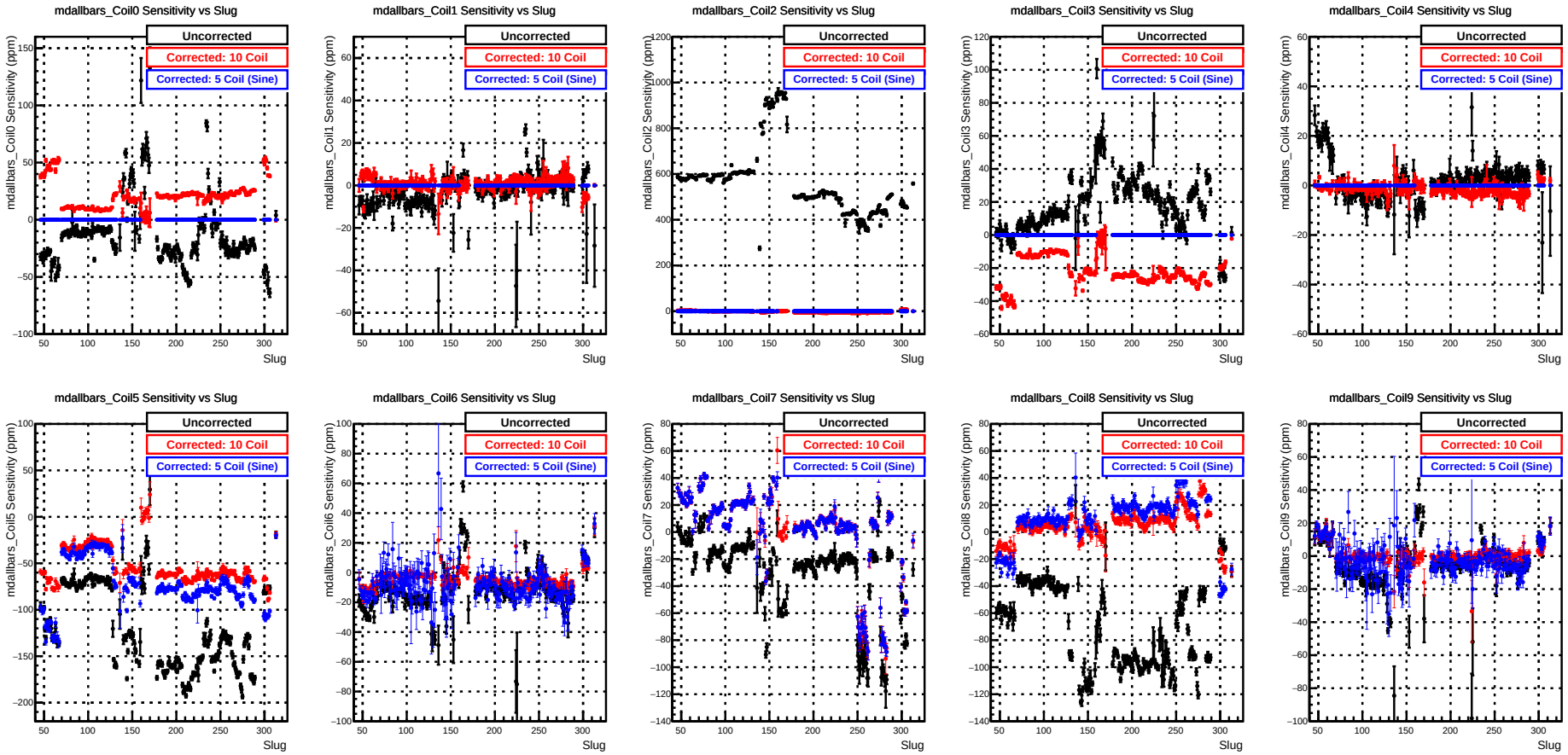

Signature of the Failure Mode

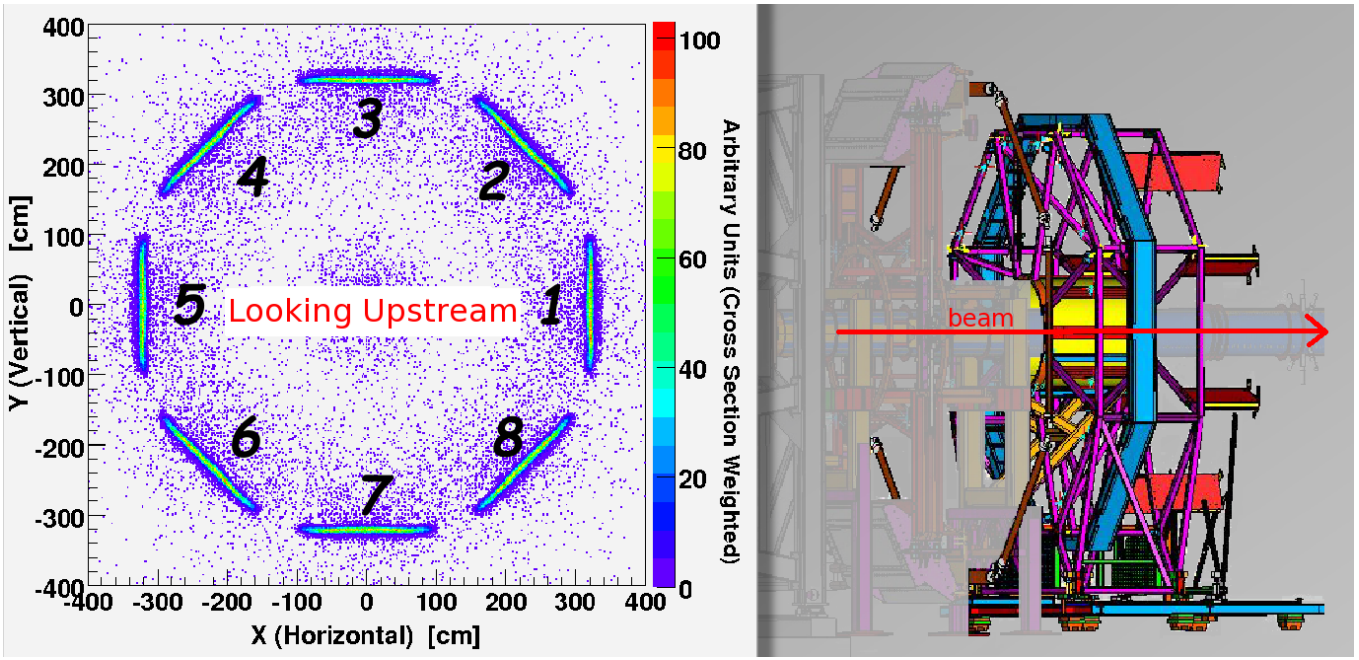

Expectations from main detector geometry

- X-Dipole: 1 and 5 most sensitive to X modulation
- Y-Dipole: 3 and 7 most sensitive to Y modulation
- Monopole: all bars equally sensitive to energy

Main Detector X-Dipoles

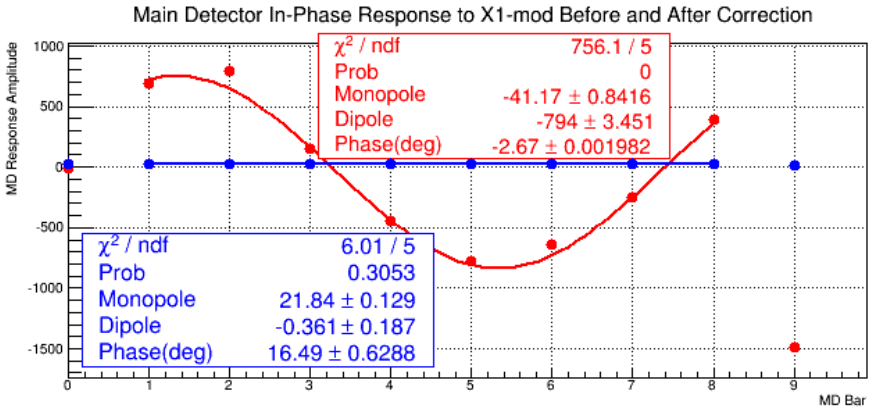

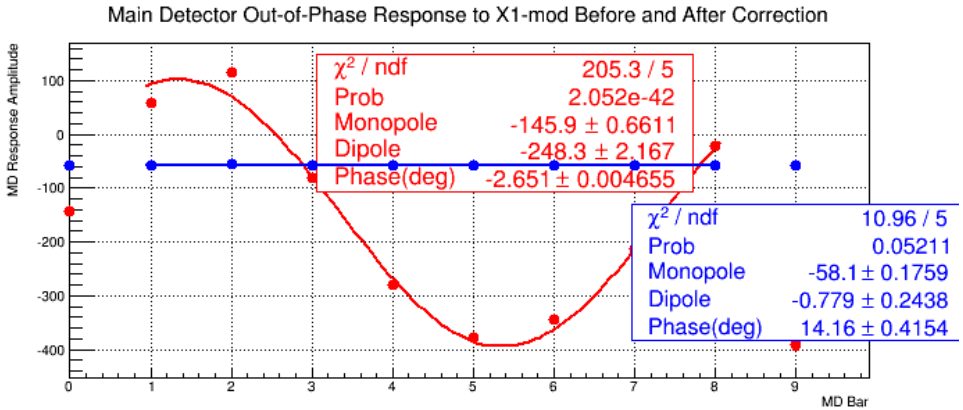

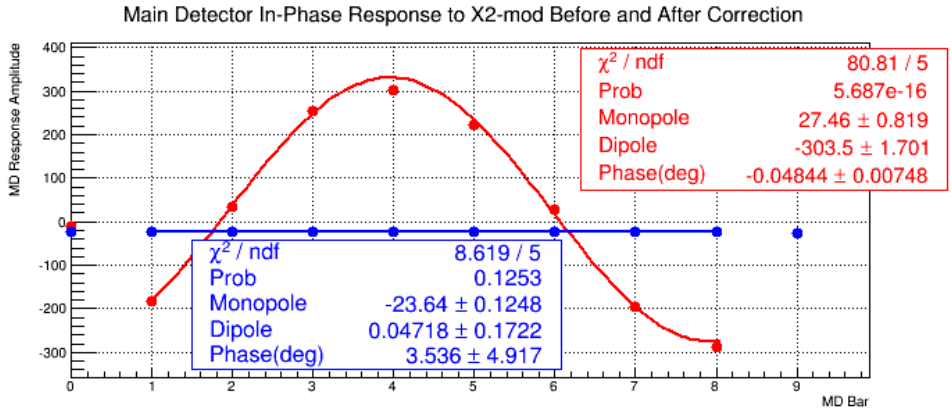

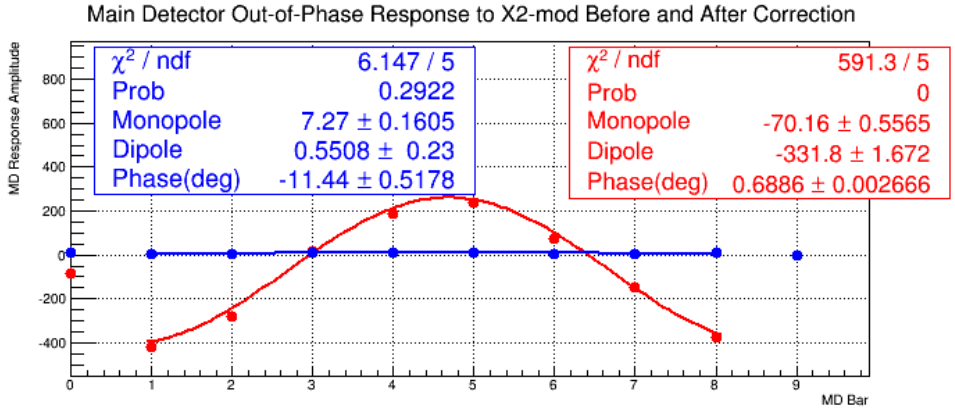

Main Detector Y-Dipoles

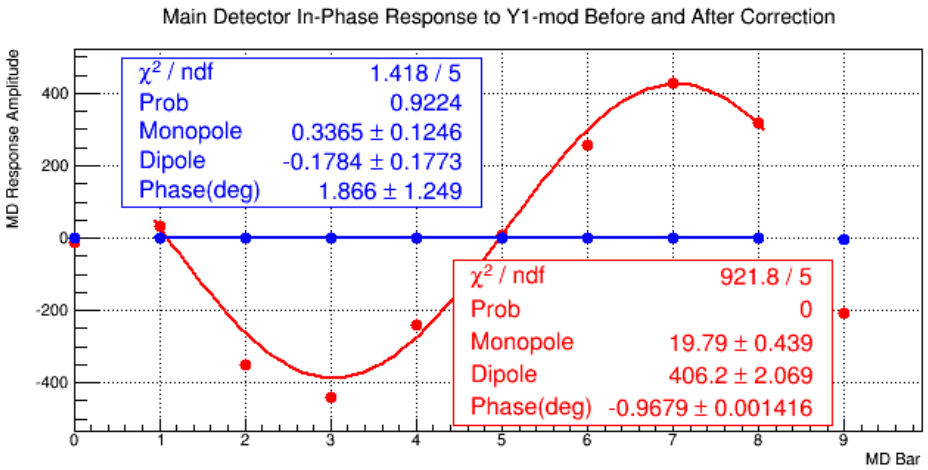

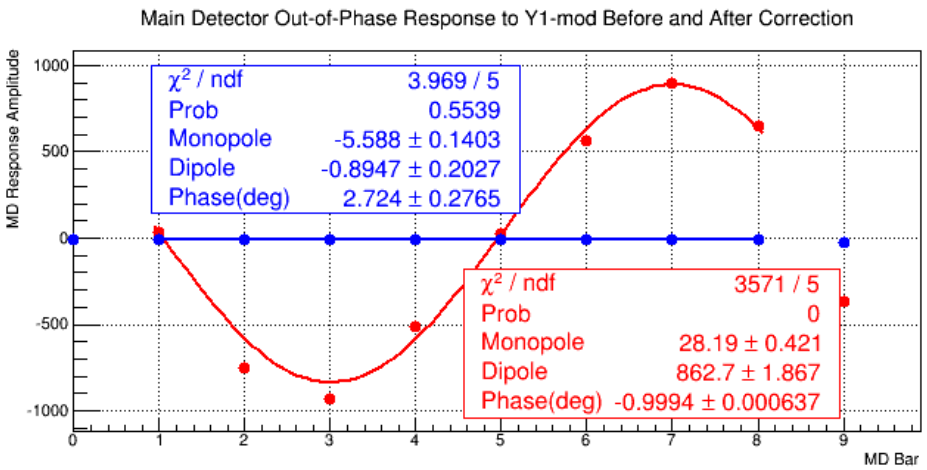

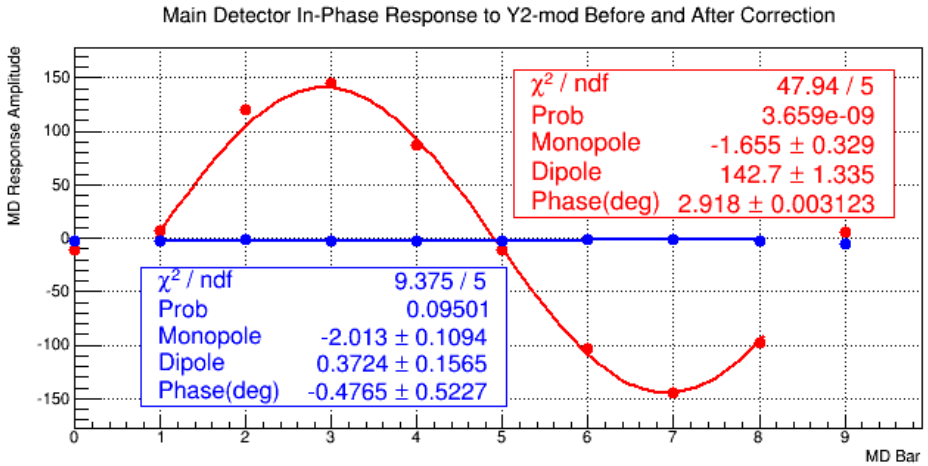

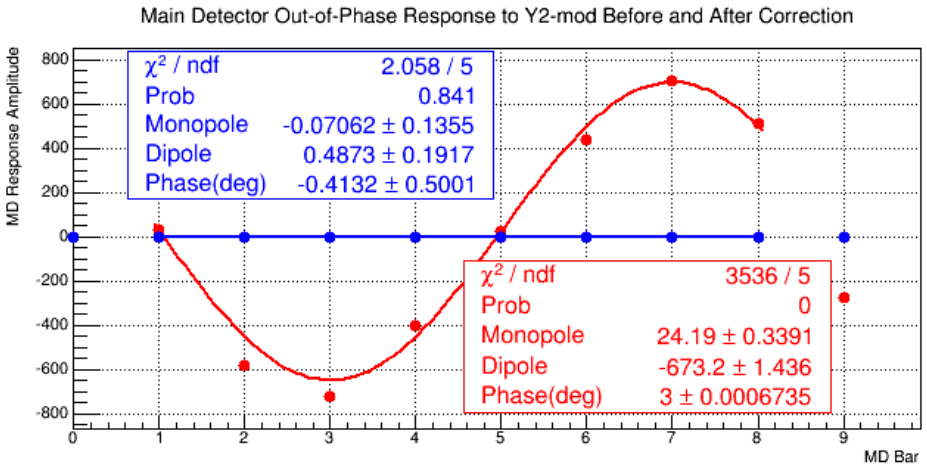

What Is Wrong?

Whatever is causing this has the signature that it affects all detectors equally. Most obvious failure modes.

- A bug in the analysis code.
  –3 independent analyses all see it
  –analyze BPM's like detector → correct well
- Electronics pickup at modulation frequency.
  –not seen in null channels
  –not seen in BPM correction analysis
- Charge is modulating.
  –real charge modulation? Detectors normalized to charge so have to be 2nd order
  –adding charge as a 6th correction parameter did not fix residual problem –spurious BCM signal modulation? Analysis with unnormalized detectors had same residual problem
- Energy correction is wrong.
- 6th unknown degree of freedom invisible to BPM's (beam spot size or halo modulation).

Energy Correction Wrong?

Wrong energy correction not the issue for 3 reasons

1. Energy signature not monopole as might be naively expected.
2. Energy monitors with Horizontal and Vertical dispersion and well separated in Z give same energy correction.
3. BPM's including those in dispersive regions correct well with same modulation analysis.

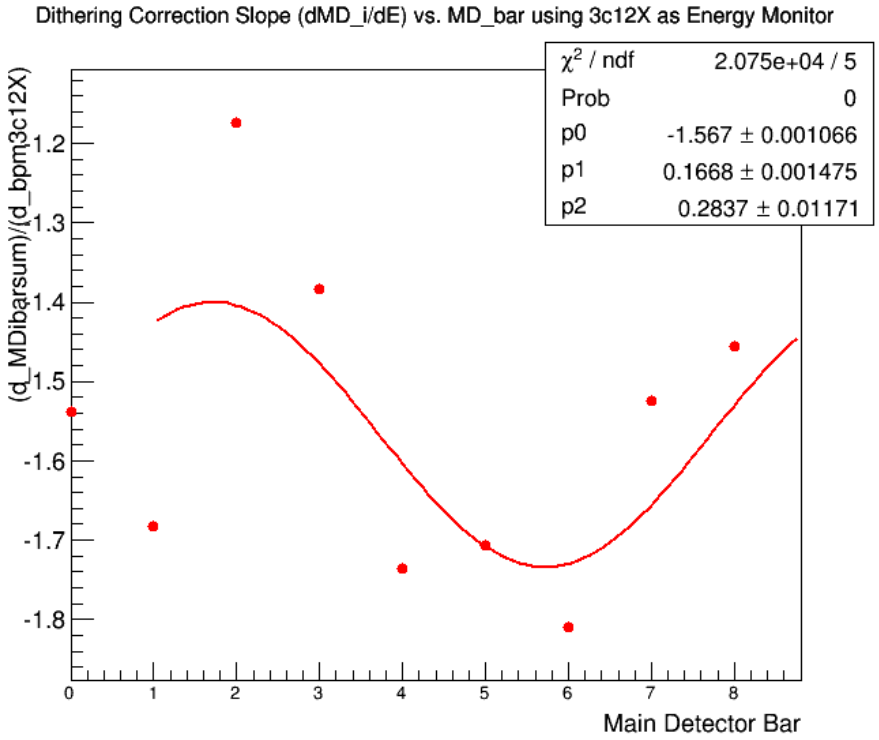

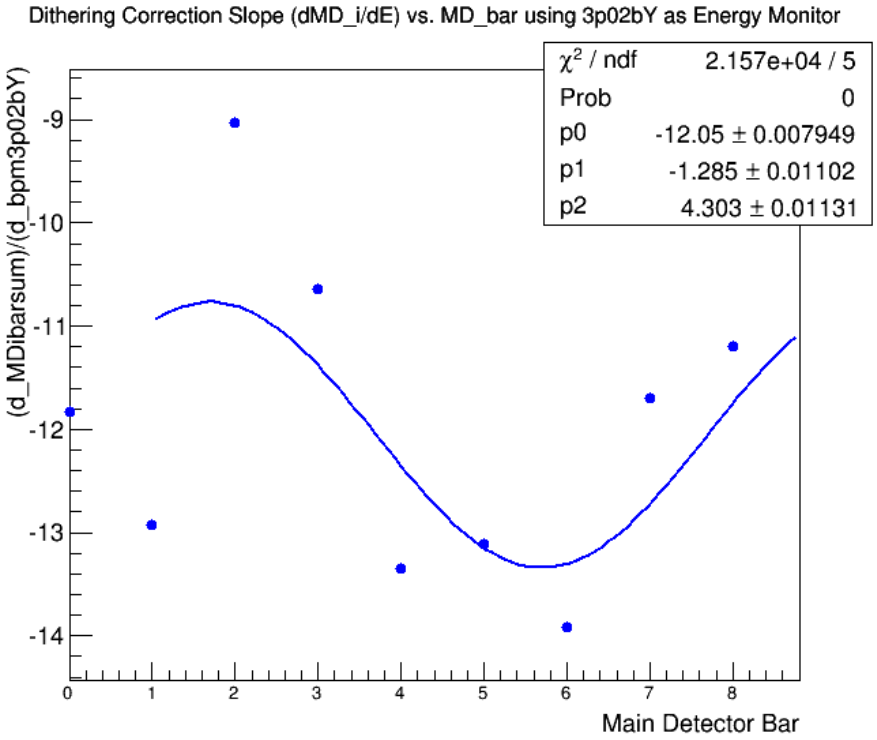

A Model I Can't Rule Out

Spot size or halo modulation

- Eg. Created by non-linear optics region in beam line, quadrupole picking up modulation signal from trim card, or deformation of dipole field in a modulation coil (short?)
- Accessed primarily by 1 type of X modulation
- Interacting in tungsten collimator and creating diffuse background seen equally by all detectors

Where to go from here?

Solution to Inconsistency
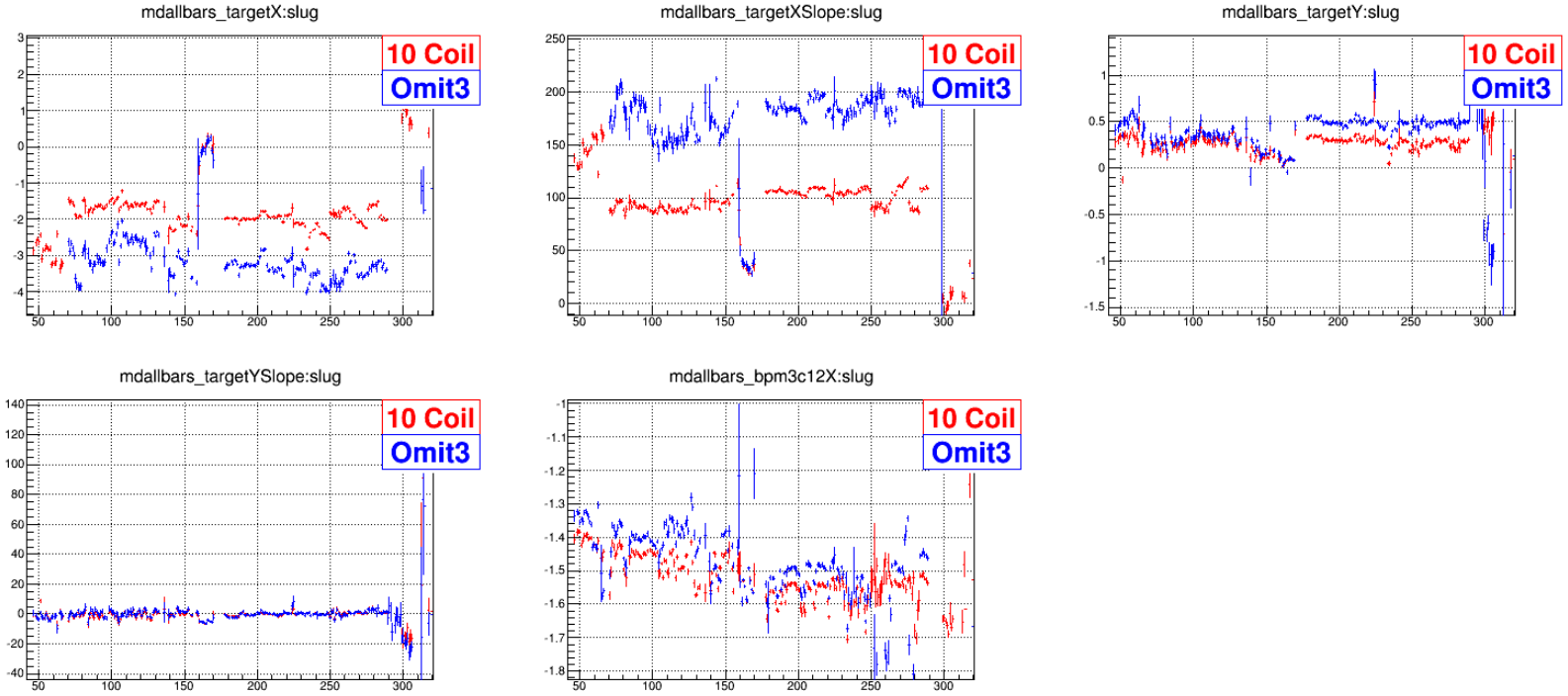
- Utilize coil redundancy to check consistency in physics results
  1. Removing single coils and coil pairs and redo analysis
  2. Verify consistency of prescribed corrections.
  3. Isolate problem if possible.
- Found average corrections in Y direction always consistent with full data set.
- Omitting one type of X modulation (Coil 3) gave extremely variant results but yielded smaller residual sensitivity to modulation.